Geological Quarterly, 2002, **46** (1): 1–23

Evidence of oxidation of the Kupferschiefer in the Lubin-Sieroszowice deposit, Poland: implications for Cu-Ag and Au-Pt-Pd mineralisation

Sławomir OSZCZEPALSKI, Grzegorz J. NOWAK, Achim BECHTEL and Karel ZÁK

Oszczepalski S., Nowak G. J., Bechtel A. and Zák K. (2002) — Evidence of oxidation of the Kupferschiefer in the Lubin-Sieroszowice deposit, Poland: implications for Cu-Ag and Au-Pt-Pd mineralisation. Geol. Quart., **46** (1): 1–23. Warszawa.

In the western part of the Lubin-Sieroszowice mining district, processes of secondary oxidation of the Kupferschiefer sediments have led to the formation of the Rote Fäule hematitic footwall alteration and resulted in a unique Kupferschiefer profile clearly comprising reduced, transitional and oxidised rocks. Redox zones were identified by petrographic, geochemical and stable isotope studies of selected core and mine sections. The vertical petrographic and geochemical zonation of the Kupferschiefer sections implies that this variation is the result of an ascending flow of hydrothermal oxidising fluids through the basal part of the Zechstein sediments. The upward, cross-formational flow and water-rock interaction resulted in the oxidation of the initially reduced Kupferschiefer shales that led to the destruction and leaching of unstable components, leaving only refractory and immobile constituents behind within the Rote Fäule. The oxidised rocks are characterised by an abundance of ferric Fe oxides, the presence of gold in association with hematite, high concentrations of aromatic hydrocarbons and asphaltenes, the lowest $\delta^{13}C$ and $\delta^{18}O$ values in carbonates and the highest $\delta^{34}S$ values in disseminated sulfides. The residual organic matter is significantly depleted in bitumen and hydrogen, and characterised by the absence of alginite and sporinite, low collinite and bituminite contents, and a high relative proportion of solid bitumen. A considerable loss of pyrite and base metals coincides with organic matter degradation. The association of Au-Pt-Pd mineralisation with the oxidised rocks, and Cu-Ag ores with the reduced sediments implies that the processes forming the Rote Fäule were paralleled by sulfide mineralisation. The Rote Fäule/ore system developed as post-sedimentary event caused by large-scale flow of metal-bearing fluids from the underlying Rotliegend aquifer.

Sławomir Oszczepalski, Polish Geological Institute, Rakowiecka 4, PL-00-975 Warszawa, Poland, e-mail: sosz@pgi.waw.pl; Grzegorz J. Nowak, Polish Geological Institute, Lower Silesian Branch, Jaworowa 19, PL-53-122 Wrocław, Poland, e-mail: gjnowak@pigod.wroc.pl; Achim Bechtel, Mineralogisch-Petrologisches Institut, Universität Bonn, Poppelsdorfer Schloss, D-53115 Bonn, Germany, e-mail: bechtel@mail.min.uni-bonn.de; Karel Zák, Czech Geological Survey, Klárov 3, 118-21 Praha, Czech Republic, e-mail: zak@cgu.cz. *(received: April 6, 2000; accepted: November 5, 2001).*

Key words: Lubin-Sieroszowice, Kupferschiefer, Rote Fäule, copper deposit, oxidation, organic matter, stable isotopes, Cu-Ag ores, Au-Pt-Pd mineralisation.

INTRODUCTION

The genesis of the Rote Fäule footwall alteration and related Kupferschiefer-type polymetallic mineralisation of central Europe is controversial. The Rote Fäule formation has been interpreted as syn-depositional or post-depositional, as reviewed by Rydzewski (1978), Oszczepalski (1989), Vaughan *et al.* (1989), Kucha (1995) and Speczik (1995). The richest copper-silver orebodies were formed in the vicinity of oxidised facies (Rydzewski, 1969; Rentzsch, 1974). Such a location of deposits indicates that the formation of the Rote Fäule/ore system occurred on a regional scale and was related to large-scale flow of metalliferous fluids, concentrating metals at redox-type geochemical traps. While ore-forming processes are known to alter primarily reduced rocks, the interaction of metal-bearing fluids with Kupferschiefer reduced sediments might be expected to have oxidised the organic matter and sulfides (Rydzewski, 1978; Jowett *et al.*, 1987; Speczik and Püttmann, 1987; Oszczepalski, 1989; Püttmann *et al.*, 1989; Kucha, 1995). The zone where the oxidation and reduction processes overlap, preserved in the form of transitional zone (TZ) between the oxidised and reduced rocks, was revealed during detailed petrographic examinations (Oszczepalski and Rydzewski, 1991; Oszczepalski, 1994). More recently, rich Rote Fäule-related Au-Pt-Pd mineralisation was found near this redox boundary in rocks previously thought to have been barren (Oszczepalski *et al.*, 1997; Piestrzyński *et al.*, 1997; Speczik *et al.*, 1997; Oszczepalski and Rydzewski, 1998).

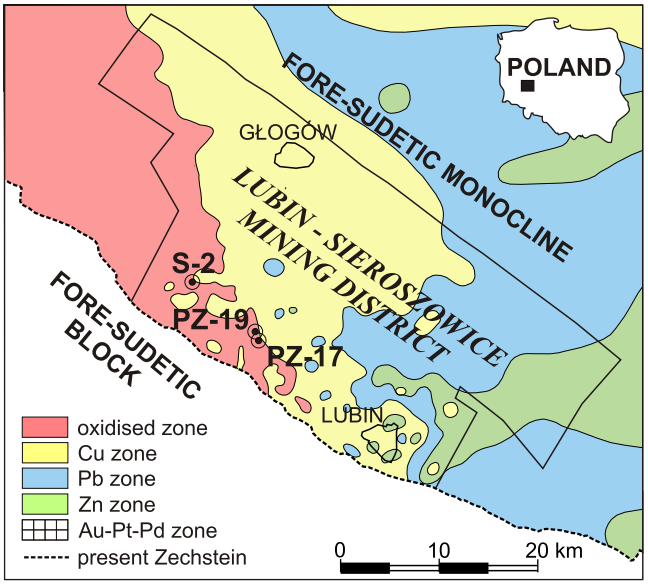

Fig. 1. Locality map showing the location of sections studied in relation to the oxidised Rote Fäule area, base metal zonation and Au-Pt-Pd prospective area in the Lubin-Sieroszowice mining district (modified after Oszczepalski and Rydzewski, 1997, 1998); extent of the oxidised Rote Fäule area relates to the Kupferschiefer unit; extent of the Au-Pt-Pd prospective area coincides approximately with the Rote Fäule within the topmost Weissliegendes

With the aim of assessing the influence of oxidation processes on the variety, distribution and formation of ore mineralisation, investigations of the contact zone between the oxidised and reduced Kupferschiefer rocks were carried out. These investigations have included work on the distribution of metals (Rydzewski, 1969; Kucha, 1981, 1990; Oszczepalski and Rydzewski, 1991, 1997; Piestrzyński and Pieczonka, 1997; Speczik *et al.*, 1997; Kucha and Przybyłowicz, 1999; Bechtel *et al.*, 2001*a*), alteration of sulfide minerals (Rydzewski, 1978; Kucha, 1981, 1995; Oszczepalski, 1989, 1994, 1999; Oszczepalski and Rydzewski, 1991; Piestrzyński *et al.*, 1997; Kucha and Przybyłowicz, 1999), the vitrinite reflectance and the maceral composition (Speczik and Püttmann, 1987; Oszczepalski, 1989; Speczik, 1994; Sun *et al.*, 1995), the type of kerogen (Püttmann *et al.*, 1991; Sawłowicz, 1991; Sun *et al.*, 1995; Sun, 1998), and the organic geochemistry (Speczik and Püttmann, 1987; Püttmann *et al.*, 1989; Sawłowicz, 1989*a*, 1991; Bechtel and Püttmann, 1991; Sun and Püttmann, 1997; Sun, 1998; Bechtel *et al.*, 2000*a*, 2001*b*). Previous studies have also considered the sulfur, carbon and oxygen isotopes in carbonates and organic matter of the oxidised rocks (Rösler *et al.*, 1968; Sawłowicz, 1989*b*; Hammer *et al.*, 1990; Bechtel and Püttmann, 1991; Püttmann *et al.*, 1993; Bechtel *et al.*, 2000*a*).

The geochemistry and petrology of the organic matter from oxidised Polish Kupferschiefer has been investigated only sporadically and locally. Until now, the oxidised rocks of the Polish Kupferschiefer series have been examined in detail in the Konrad mine profile (North Sudetic Trough), with analyses of petrography, organic geochemistry, and carbon and oxygen isotopes (Speczik and Püttmann, 1987; Püttmann *et al.*, 1989, 1991, 1993; Speczik, 1994; Sun *et al.*, 1995). A smaller range of examinations was made on the Lubin-Sieroszowice deposit; only selected samples of the oxidised rocks (Sawłowicz, 1989*a*, *b*, 1991; Bechtel *et al.*, 2000*a*), the Polkowice mine section (more precise location unknown; Sun, 1998) and two other boreholes (Bechtel *et al.*, 2001*b*) were examined. However, samples collected by Sawłowicz (1989*a*) do not strictly conform to typical Rote Fäule specimens, due to high C_{org} contents of 1.8–7.7% and the lack of ferric Fe oxides. Investigations of sulfur isotopes have been performed for various regions of Poland, including the area of the Lubin-Sieroszowice deposit, but only for the reduced rocks (Harańczyk, 1986; Sawłowicz, 1989*c*; Jowett *et al.*, 1991*a*, *b*; Wodzicki and Piestrzyński, 1994).

The fundamental aim of this study was to present petrographic, chemical and isotopic evidence of oxidative alteration of the Kupferschiefer. The study area located in the western part of the Lubin-Sieroszowice mining district was chosen to characterise the Kupferschiefer shales occurring between the oxidised and reduced rocks. Comparison of data on the sulfides and iron oxides, maceral composition, geochemical indices, and the C, O and S isotopes, indicating the influence of the oxidative alteration on the mineralised sediments, was performed. These records address questions about the direction of flow of the mineralising fluids, the post-depositional metal redistribution, and the formation of Cu-Ag and Au-Pt-Pd mineralisation.

MATERIALS AND METHODS

The study area is situated on the contact of the oxidised and reduced facies, where the mineralisation is dominated by ferric iron oxides at the Rote Fäule side and Cu-S type sulfides at the reduced side (Fig. 1). In this area, the oxidised and reduced lithologies interfinger, so that the Kupferschiefer profiles consist of reduced, transitional and oxidised rocks (Fig. 2). The Kupferschiefer samples were collected from selected PZ-17 and PZ-19 mine profiles (depth 790 m), and S-2 borehole (depth 644 m). The oxidised rocks (red calcareous clayey shales, mineralised with Fe^{3+} oxides) are developed at the base of the Kupferschiefer. The upper part of the oxidised complex is referred to as a transitional zone (grey dolomitic clayey shales with a small amount of organic material, minor ferric Fe oxides and relics of sulfides). The top of the Kupferschiefer comprises the reduced rocks (black dolomitic clayey shales rich in organic matter and sulfides).

The petrographic examinations of ores and iron oxides were performed with a *Leitz* microscope. Visual kerogen analysis was done via organic petrology methods in reflected normal and ultraviolet light following recommended procedures (*International...*, 1993). A *Carl Zeiss MPM-200* optic-electronic set (Axioscope microscope, HBO lamp emitting shortwave ultraviolet light, microphotometer for vitrinite reflectance measurements, *Carl Zeiss Photan* program) was used.

Chemical composition was determined with an *RTG* defractor and via the WD-XRF method (*Philips WD-XRF PW 2400* spectrometer) and GF-AAS method (*Unicam Solaar 939*

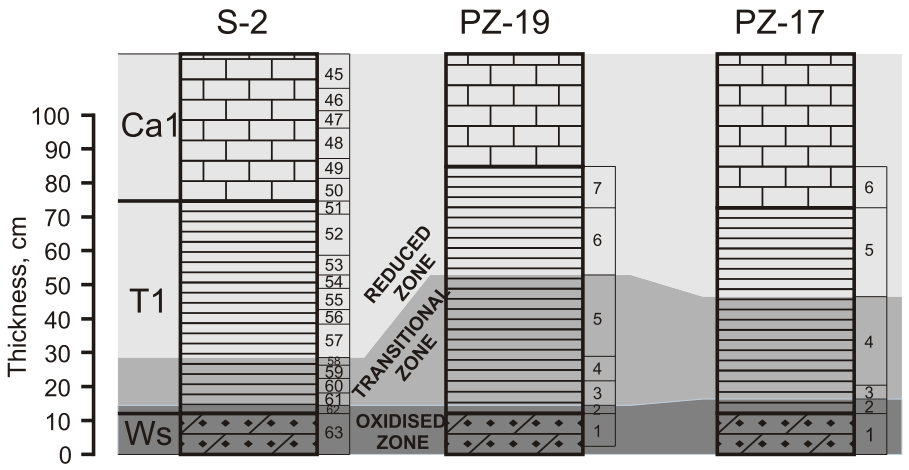

Fig. 2. Correlation of the sections studied showing position of the reduced, transitional and oxidised zones

Ca1 — Zechstein Limestone, T1 — Kupferschiefer, Ws — Weissliegendes, numbers show sample locations

QZ spectrometer). The precious metal content was performed by GF-AAS analysis (*Perkin Elmer 4100 ZL* spectrometer), and by the NiS fire assay OES-ICP method (*Jarrel Ash Enviro* and *Perkin Elmer 6000* spectometer). C_{org} content was determined by coulometric titration.

For organic geochemical analyses, finely ground shale samples (< 0.2 mm) were Soxhlet-extracted for 24 h using dichloromethane as solvent. The removal of elemental sulfur was achieved by addition of copper foil to the flask during the extraction. The total extracts (bitumen) were dissolved in *n*-hexane and asphaltenes were removed by precipitation. Hydrocarbons and resins were separated into fractions by column chromatography (SiO_2 and Al_2O_3, 1:2). The saturated hydrocarbons were eluted with *n*-hexane, the aromatic hydrocarbons with benzene and the resins with a mixture of benzene and methanol (1:1). The hydrocarbon fractions were analysed using a *Hewlett-Packard 5890 II* gas chromatograph coupled to a *GC-MSD 5971* spectrometer. The saturated compounds were qualified by adding squalane as standard prior to analysis. The aromatics were dissolved in dichloromethane. A HP-1 non-polar capillary column was used for determination of saturated hydrocarbons, and a HP-5 non-polar capillary column was applied in the study of aromatics. Mass spectra were recorded in the scan and sim mode.

Kerogen pyrolysis was carried out with a *Rock-Eval II* apparatus. The following parameters were measured: S_1 (the amount of hydrocarbons released during pyrolysis at a temperature of 300°C), S_2 (hydrocarbons expelled between 300 and 550°C), and S_3 (the amount of carbon dioxide formed during pyrolysis up to 350°C). These parameters are the basis for index calculation: HI (hydrogen index), OI (oxygen index) S_2/S_3 and KTR (kerogen transformation index = production index). The HI and OI indices reflect the values of atomic ratios of H/C and O/C in the kerogen (Tissot and Welte, 1984; Espitalie *et al.*, 1985). The HI is the amount of hydrocarbons (S_2/C_{org}) and the OI is a measure of the amount of CO_2 (S_3/C_{org}) formed during pyrolysis. Total organic carbon (TOC) is automatically computed. The temperature of maximum hydrocarbon (S_2) generation (T_{max}) was also detected. T_{max} data, however, should be interpreted with great care (Espitalie *et al.*, 1985) because samples containing less than 0.2 wt.% TOC usually provide very low amounts of hydrocarbons (S_2).

For the stable isotope determinations, CO_2 from carbonates was released by reaction with 100% H_3PO_4 under vacuum. Corrections of the $\delta^{18}O$ for higher reaction temperature and for carbonate chemistry were applied (Rosenbaum and Sheppard, 1986). For the examination of $\delta^{13}C$ values in bulk organic matter (after removal of carbonate carbon) samples were combusted in a stream of oxygen at 900°C, and CO_2 was purified by freezing traps and by reaction with silver wool at 350°C (removal of co-produced SO_2). For sulfur and oxygen isotope determination, water-soluble sulfates were separated and precipitated as $BaSO_4$ (Hall *et al.*, 1988) and sulfides (Newton *et al.*, 1995). Preparation of CO_2 and SO_2 for oxygen and sulfur isotope determination in sulfates followed methods by Sakai and Krouse (1971), and Yanagisawa and Sakai (1983). SO_2 for sulfur isotope determination in sulfides was prepared by oxidation with CuO. Measurements were done on *Finnigan MAT* 251, *Finnigan Delta*, *Micromass 602C*, and *MI-1202* mass spectrometers. Overall analytical uncertainty is within ±0.15‰ for $\delta^{13}C$ and $\delta^{18}O$ records and within ±0.3‰ for the $\delta^{34}S$.

RESULTS

CHEMICAL COMPOSITION

Ferric iron is a typical component of the oxidised Rote Fäule unit (Rydzewski, 1978; Michalik, 1979) and, as expected, the Fe_2O_3 content increases towards the oxidised rocks (Table 1). The SiO_2 and Al_2O_3 contents generally rise basewards of the Kupferschiefer, reflecting lithology and the rhythmic sedimentation, unlike CaO and MgO, the content of which increases from the sandstones upwards to the Zechstein Limestone. The MgO/CaO ratio in general decreases towards the base of the Kupferschiefer. This decrease is characteristically accompanied by a fall in the C_{org}, S_{tot} and S^{2-} content.

Table 1

Inorganic geochemical data for the Kupferschiefer ore series from S-2, PZ-17 and PZ-19 sections

Section	S-2										PZ-17					PZ-19					
Lithostr.	Ca1	T1						Ws			Ca1	T1			Ws	T1					Ws
Zone	r						t		o		r		t	o		r			t	o	
Sample	46-50	51	52-53	54-55	56	57	58	59-61	62	63	6	5	4	2	1	7	6	4	3	2	1
SiO_2%	21.90	25.60	25.00	24.90	-	23.80	30.90	23.90	41.80	54.60	-	31.27	28.71	31.55	-	-	25.20	48.05	32.75	23.67	-
TiO_2%	0.31	0.41	0.40	0.67	-	0.40	0.48	0.42	0.69	0.15	-	0.45	0.52	0.55	-	-	0.34	0.89	0.63	0.39	-
Al_2O_3%	5.50	9.10	8.50	7.90	-	8.20	11.90	8.40	14.90	3.90	-	11.47	11.47	11.37	-	-	9.23	19.06	12.28	8.59	-
Fe_2O_3%	0.86	1.26	1.17	1.11	-	1.15	1.56	1.27	1.95	0.50	-	1.96	1.68	4.93	-	-	4.48	2.35	2.27	5.23	-
MnO%	0.25	0.28	0.26	0.27	-	0.29	0.33	0.37	0.27	0.37	-	0.28	0.36	0.33	-	-	0.26	0.12	0.32	0.42	-
MgO%	11.50	10.20	9.86	9.25	-	9.29	6.29	7.72	3.49	4.29	-	5.15	6.36	7.19	-	-	4.54	3.56	7.17	8.75	-
CaO%	20.50	15.20	14.90	15.90	-	15.30	18.30	23.40	12.90	14.90	-	22.09	21.36	17.26	-	-	26.49	7.06	17.13	20.18	-
Na_2O%	0.16	0.20	0.20	0.19	-	0.19	0.20	0.21	0.24	0.11	-	0.44	0.39	0.36	-	-	0.40	0.92	0.59	0.53	-
K_2O%	1.77	2.82	2.66	2.58	-	2.57	3.59	2.68	4.79	1.42	-	2.77	3.00	3.01	-	-	2.06	5.41	3.23	2.20	-
C_{org}%	0.23	2.06	2.14	3.64	-	3.25	0.30	0.30	0.29	-	-	7.15	2.19	0.52	-	-	4.46	3.33	0.91	0.07	-
S_{tot}%	1.63	1.02	1.58	1.62	-	1.49	0.14	0.16	0.04	0.02	-	1.60	0.12	0.10	-	-	1.69	0.20	0.11	0.02	-
S^{2-}%	0.75	0.76	0.99	0.89	-	1.33	0.05	0.05	0.00	0.00	-	1.32	0.11	0.02	-	-	1.50	0.09	0.00	0.00	-
Cu%	3.800	5.400	4.900	4.230	4.428	4.910	0.077	0.041	0.019	0.034	0.420	8.578	0.216	0.177	0.010	0.170	9.097	0.336	0.045	0.007	0.007
Ag ppm	15	17	16	23	28	28	4	2	1	2	12	92	4	3	1	18	190	7	1	1	1
Co ppm	4	35	45	48	35	55	9	6	9	3	-	125	10	10	-	-	51	12	9	5	-
Ni ppm	10	97	127	146	115	162	45	30	54	11	-	201	45	32	-	-	145	75	43	12	-
Mo ppm	5	60	70	50	37	40	10	10	10	20	-	200	10	8	-	-	207	9	3	1	-
Pb ppm	28	26	26	23	14	16	30	7	10	4	-	721	64	31	-	-	169	49	36	119	-
Zn ppm	23	30	29	28	45	28	36	33	43	11	-	192	36	24	-	-	50	63	30	26	-
V ppm	60	240	460	810	525	830	1310	2050	1410	80	-	1504	1272	666	-	-	1075	2090	774	48	-
Cr ppm	38	168	149	145	101	153	177	136	273	21	-	138	81	170	-	-	120	181	183	28	-
U ppm	162	317	300	18	-	418	633	933	783	550	-	14	15	11	-	-	16	31	22	2	-
As ppm	25	33	31	61	94	41	19	19	32	14	-	-	-	-	-	-	-	-	-	-	-
Ta ppb	-	-	-	-	-	-	-	-	-	-	-	1995	55	42	-	-	1964	93	13	4	-
Hg ppb	400	280	1010	960	-	720	10	10	130	20	370	715	1750	450	180	160	2770	1160	203	186	190
Au ppb	1	1	1	1	2	11	104	81	18	3	11	30	1157	13653	4264	11	66	4141	1431	1527	6990
Pt ppb	-	-	-	-	5	3	500	431	681	21	3	3	76	708	25	3	5	839	834	381	23
Pd ppb	-	-	-	-	38	2	219	336	981	82	2	2	13	528	41	2	4	109	317	281	40
Co/Ni	0.40	0.36	0.35	0.33	0.30	0.34	0.20	0.20	0.17	0.27	-	0.62	0.22	0.31	-	-	0.35	0.16	0.21	0.42	-
K_2O/Na_2O	11.06	14.10	13.30	13.57	-	13.52	17.95	12.76	19.96	12.90	-	6.30	7.69	8.36	-	-	5.15	5.88	5.47	6.04	-
Fe_2O_3/C_{org}	3.74	0.61	0.55	0.49	-	0.35	5.20	4.23	6.72	-	-	0.27	0.77	9.48	-	-	1.00	0.70	2.49	74.71	-
MgO/CaO	0.56	0.67	0.66	0.58	-	0.61	0.34	0.33	0.27	0.29	-	0.23	0.30	0.42	-	-	0.17	0.50	0.42	0.43	-
V/Cr	1.6	1.4	3.1	5.6	5.2	5.4	7.4	15.1	5.2	3.8	-	10.9	15.7	3.9	-	-	9.0	11.5	4.2	1.7	-

Ca1 — Zechstein Limestone, T1 — Kupferschiefer, Ws — Weissliegendes; r — reduced zone, t — transitional zone, o — oxidised zone

There is an interestingly high K_2O content (in the range 2.2 to 5.4%) in the TZ and oxidised rocks as compared to the reduced rocks (2.1–2.8%). In the entirely reduced Kupferschiefer profiles, the C_{org} value changes rhythmically, generally rising towards the base, reflecting the rhythmic Kupferschiefer sedimentation. This trend is clearly disrupted in sections containing both reduced and oxidised rocks (Table 1). The reduced rocks in such profiles usually contain significantly more than 2% C_{org}, while the oxidised rocks are poor in organic material and do not contain more than 0.5% C_{org}. Only samples from the top of TZ may contain up to 3.3% C_{org}. Total sulfur was found to range from 1–2% in the reduced samples to less than 0.2% in the oxidised rocks.

The concentrations of most of the metals (Cu, Ag, Pb, Zn, Co, Mo, Ni, Ta, and As) rise from the top of the profile to the base within the reduced zone, followed by an abrupt decline within the TZ reaching their minimum values in oxidised rocks, whereas the contents of Au, Pt and Pd rise in the transitional and adjacent oxidised rocks (Table 1, Fig. 3). The variability in V, Hg, and U contents is quite significant, although increases in their content occur mostly in the uppermost part of TZ and in adjacent reduced rocks.

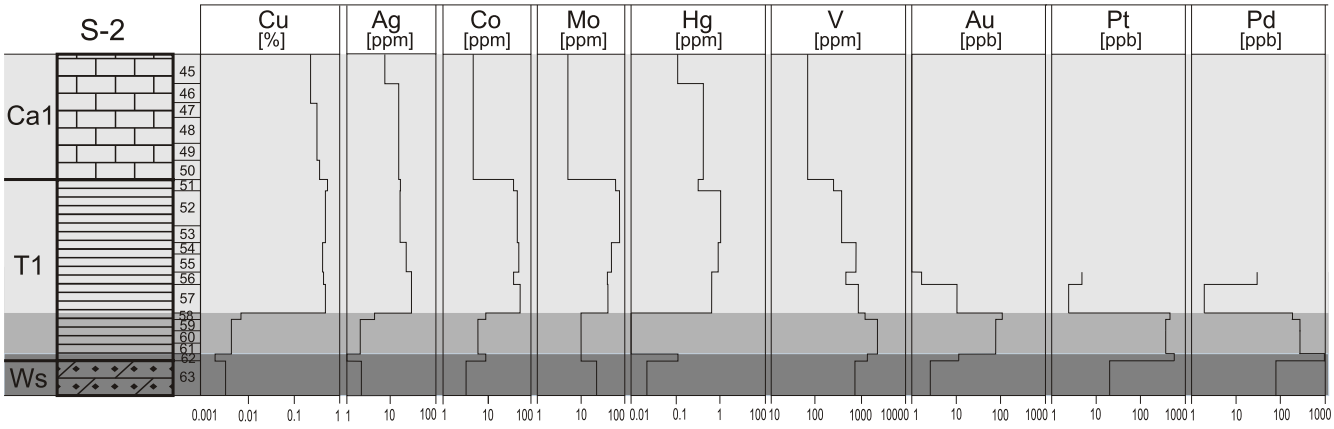

Fig. 3. Variation of Cu, Ag, Co, Mo, Hg, V, Au, Pt and Pd in the S-2 section

PETROGRAPHIC EXAMINATION

The petrographic studies indicate a vertical succession in the mineralisation from the base of the oxidised rocks to the reduced rocks at the top of the Kupferschiefer profile (Fig. 4). This sequence is manifested with the presence of hematite (including pseudomorphs after pyrite framboids) and relict sulfides with hematite haloes in the oxidised rocks, and Cu-S type mineralisation at the bottom of the reduced zone. The topmost part of the reduced shales contains the Cu-Fe-S type sulfides in association with framboidal pyrite.

A characteristic feature of the oxidised rocks is the intensive iron oxide mineralisation. The ferric Fe oxides are present as irregular grains and as a pigment scattered through the matrix or concentrated in the form of aggregates or bands. In the oxidised rocks, rare sulfides are dispersed and represented only by fine relics (mainly of covellite, digenite and chalcopyrite) surrounded by invading iron oxides. A few gold grains of 10–30 μm in size were identified. It was shown that the high concentrations of gold are seen as native gold in the form of intergrowths with hematite, covellite, bornite and chalcocite; the native gold, hematite and sulfides contain elevated concentrations of Pt and Pd (Piestrzyński *et al.*, 1997; Piestrzyński and Pieczonka, 1997).

The presence of both scattered iron oxides and remnant sulfides (covellite, pyrite and marcasite, minor chalcocite, bornite and chalcopyrite) characterises the TZ. Typically, Cu-sulfides have hematite pigment haloes. The topmost transitional samples are slightly enriched (relative to the oxidised rocks) in the copper content in the 0.05 to 0.5% range. There are numerous iron oxide pseudomorphs after framboidal pyrite, aligned parallel to the shale lamination, which likens the TZ to the oxidised rocks. The amount of these pseudomorphs increases towards the bottom of the TZ. The presence of electrum and native gold in paragenesis with hematite, chalcocite, digenite, bornite, chalcopyrite and clausthallite seems to be characteristic for the TZ (Piestrzyński *et al.*, 1997, Piestrzyński and Wodzicki, 2000).

The reduced facies of the studied profiles contain rich copper mineralisation represented by chalcocite and accompanied by bornite, digenite and covellite (Fig. 4). A significant part of the base metal sulfides are present in the form of fine, scattered grains (< 50 μm in diameter), which are aligned parallel to the shale lamination. The abundance of framboidal forms of the copper sulfides (chalcopyrite and digenite) draws particular attention. Ores more rarely appear in the form of coarse-grained aggregates and veins. Pyrite, which is absent at the base of the reduced zone, appears in small amounts (mainly as framboids) in the topmost parts of the Kupferschiefer.

Among the organic constituents, liptinites (alginite, liptodetrinite, bituminite and sporinite) and unstructured organic matter (UOM) are the dominant kerogen components in the rocks studied, whereas vitrinites are less abundant and inertinite is a minor component (Table 2; Fig. 5). In relation to the redox of the host rocks, alginites, liptodetrinites, sporinites, bituminites and collinites are mostly abundant in the reduced samples, as opposed to the oxidised samples, which are dominated by UOM.

Liptinites comprise a class of lipid-rich macerals that include waxes, resins, spores, cuticles and algal bodies (Tissot and Welte, 1984). Alginite, observed solely in the reduced and weakly oxidised rocks, combines both algae and algal material. Two types of alginite have been distinguished: alginite A — telalginite and B — lamalginite (Taylor *et al.*, 1998; Robert, 1981). Telalginite (mainly tasmanite) is present as fine disc-shaped structures with weak yellow fluorescence (Fig. 6c). Lamalginite forms thin, laterally extensive laminae and flat lenses built of lamellar algal material, which have a weak to moderate yellow-to-orange fluorescence (Fig. 6b). Algal liptinites, dominated by lamalginite, represents a product of bacterial decomposition of phytoplankton, algae and bacterial biomass in an oxygen-deficient environment (Teichmüller, 1986). Liptodetrinite consists of liptinite fragments that exhibit a yellow-to-orange fluorescence, linking the liptodetrinite to the alginite. Sporinite is found chiefly as thin-walled miospores (tenuisporinite) displaying elongated shapes and intensive yellow to orange fluorescence colours, darker than those shown by alginite.

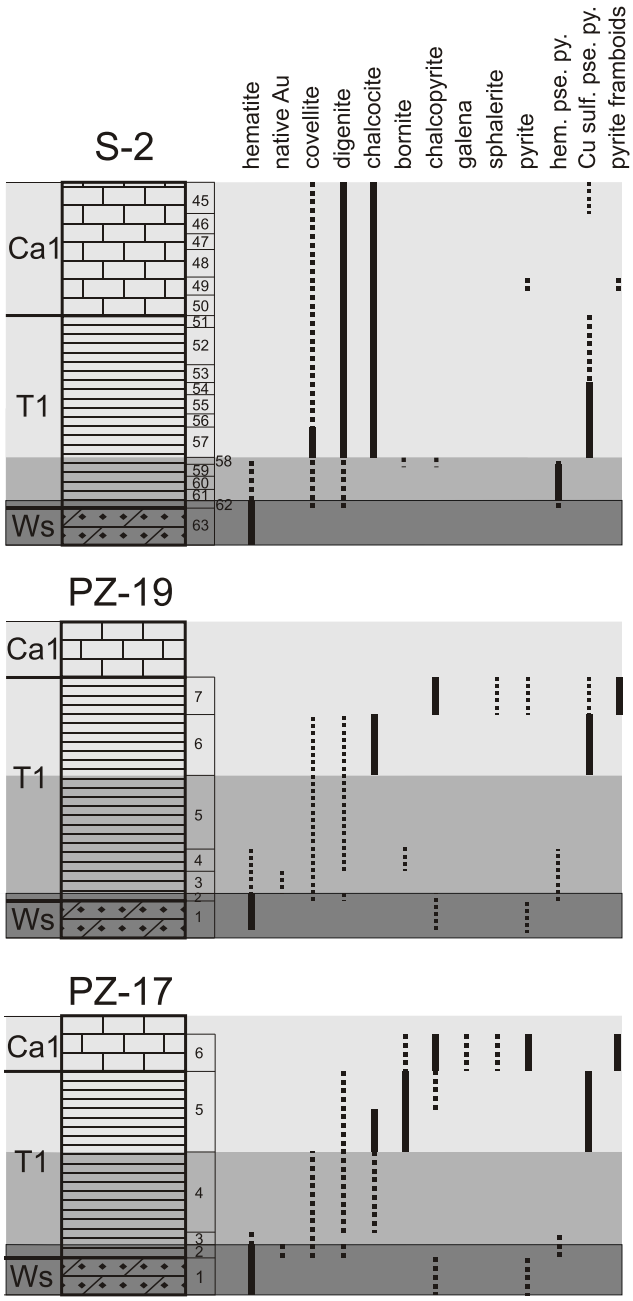

Fig. 4. Distribution of the iron oxides and sulfides within the S-2, PZ-19, and PZ-17 sections

hem. pse. py. — hematite pseudomorphs after framboidal pyrite; Cu sulf. pse. py. — copper sulfide pseudomorphs after framboidal pyrite; line indicates content > 2 vol.%, whereas dots indicate subordinate content

The bituminite is included in the group of liptinitic vitrinite-like unstructured organic constituents (Koch, 1997). Although the vitrinite-like bituminite is not included in the internationally accepted classification of bituminite (Teichmüller and Ottenjann, 1977; ICCP, 1993), based on its optical properties, it mostly corresponds to bituminite III (Teichmüller and Ottenjann, 1977) and to non-fluorescing unstructured organic matter (Taylor *et al.*, 1998). It occurs in the form of thin bands and lenses concordant to the shale lamination (Fig. 6a), or it forms fine scattered structures resembling micrinite. It is characterised by a black-brown colour, an absent or a weak fluorescence and a reflectance in the range R_o of 0.4–0.6%, lower than for the vitrinite but higher relative to UOM. The origin of bituminite is uncertain. The alignment (parallel to the lamination) of the alginite, bituminite and most of the amorphous material, and pyrite framboids intergrown with these components, appears to imply that these materials were synsedimentary and of sapropelic character, deposited in anoxic conditions. Some bituminite macerals intimately associated with alginite can be considered as structurally degraded (amorphous) liptinite or its residue after oil generation.

UOM comprises amorphous material (AOM) and solid bitumen (SB). AOM predominantly occurs within the reduced shales, and SB in the oxidised varieties. Both of these components are intimately associated with mineral constituents, forming a bituminous-mineral matrix with a strong yellow fluorescence (*cf.* Teichmüller and Ottenjann, 1977). AOM can be found in the form of elongated fine lenses, irregular bands, and agglomerates of irregular shapes without clear contours, or in scattered form. This material exhibits a dark yellow and light brown fluorescence (weaker fluorescence vs. alginite), and is grey in normal reflected light, darker than bituminite. The majority of the UOM represents secondary material from the diagenetic alteration of the marine and nonmarine organic components. The characteristics of AOM make it similar to bituminite I (Teichmüller and Ottenjann, 1977). The solid bitumen is apparently distinguishable by ultraviolet irradiation, showing yellow and orange fluorescence (*cf.* Jacob, 1989; Landis and Castano, 1994). It is dispersed in the intergranular pores of fine terrigenous material and carbonates or forms rims on detrital grains. As suggested earlier (Sun *et al.*, 1995), the low reflectance of SB (< 0.6% R_o) indicates that a significant proportion of UOM exists as migrabitumen (Jacob, 1989).

Vitrinite (collinite, vitrodetrinite) is a common component of the examined samples, though minor in terms of amount (Table 2; Fig. 6a, b, d). Collinite, the structureless vitrinite variety, preferentially appears in the reduced and slightly oxidised rocks as thin (up to 35 μm thick) laminae aligned parallel to the shale lamination. Collinite commonly accompanies alginite, bituminite and AOM. Collinite in blue-light-induced fluorescence is black, though locally displays very weak fluorescence, presumably caused by impregnation with lipoidal matter. Corpocollinite was found locally. Surface perforation of the collinite macerals and no evidence of recycling suggest that they are primary ("autochthonous") particles, embedded initially as reactive and metabolisable humic material within the liptinite-rich marine matter and preserved in a very low energy, anoxic environment. By contrast to collinite, vitrodetrinite has the form of oval-shaped bodies and irregular particles (1–15 μm in size) of smooth surface and very high reflectance (0.94–3.11% R_o). Some of the vitrodetrinite fragments have oxidation rims. Inertinite (mainly inertodetrinite) occurs in small amounts in all samples studied (Fig. 6c, d) as fusinite and semifusinite fragments, fusinited algae and spores, and chitinous insect particles.

Table 2

Vitrinite reflectance and organic constituents of the Kupferschiefer samples from the S-2, PZ-17 and PZ-19 sections

Section	Sample	Zone	Vitrinite reflectance R_o [%]		Organic constituents [vol. %]							
					Vitrinite		Liptinite				UOM	Inertinite
			Col	Vtd	Col	Vtd	Al	Bt	Lpd	Sp	AOM+SB	Ind
S-2	54	r	0.72	1.02-1.40	<1.0	3.6	18.8	54.4	7.6	6.0	7.6	2.0
	57	r	0.82	1.12-1.52	3.6	2.4	14.8	52.8	11.6	4.0	6.8	4.0
	58	t	0.72	0.94-1.58	3.6	3.6	17.2	51.2	8.4	5.2	5.6	5.2
	59	t	1.10	1.62-3.11	<1.0	3.2	-	2.8	-	-	91.2	2.8
	61	o	-	-	-	6.0	-	15.0	11.0	-	65.0	3.0
PZ-17	5	r	0.76	1.07-1.56	8.8	0.4	30.4	14.8	14.4	1.2	26.4	3.6
	4	t	0.89	1.11-1.67	10.0	2.4	-	67.6	2.4	0.8	12.4	4.4
	3	t	1.13	1.02-1.34	5.2	11.2	-	6.8	26.8	0.4	47.2	2.4
	2	o	1.05	1.32-1.61	1.2	5.2	-	0.8	5.2	-	86.0	1.6
PZ-19	6	r	0.86	1.03-1.63	3.2	5.2	11.6	48.0	9.2	4.4	14.4	4.0
	5	t	0.90	1.05-1.37	2.8	6.4	-	76.0	2.4	-	8.0	4.4
	3	t	0.98	1.08-2.05	3.2	8.8	-	13.6	3.6	0.4	68.4	2.0
	2	o	1.03	1.21-1.58	1.6	11.6	-	11.6	5.2	-	65.6	4.4

r — reduced zone, t — transitional zone, o — oxidised zone; Col — collinite, Vtd — vitrodetrinite, Lpd — liptodetrinite, Sp — sporinite, Al — alginite, Bt — bituminite, UOM — unstructured organic matter, AOM — amorphic organic matter, SB — solid bitumen, Ind — inertodetrinite

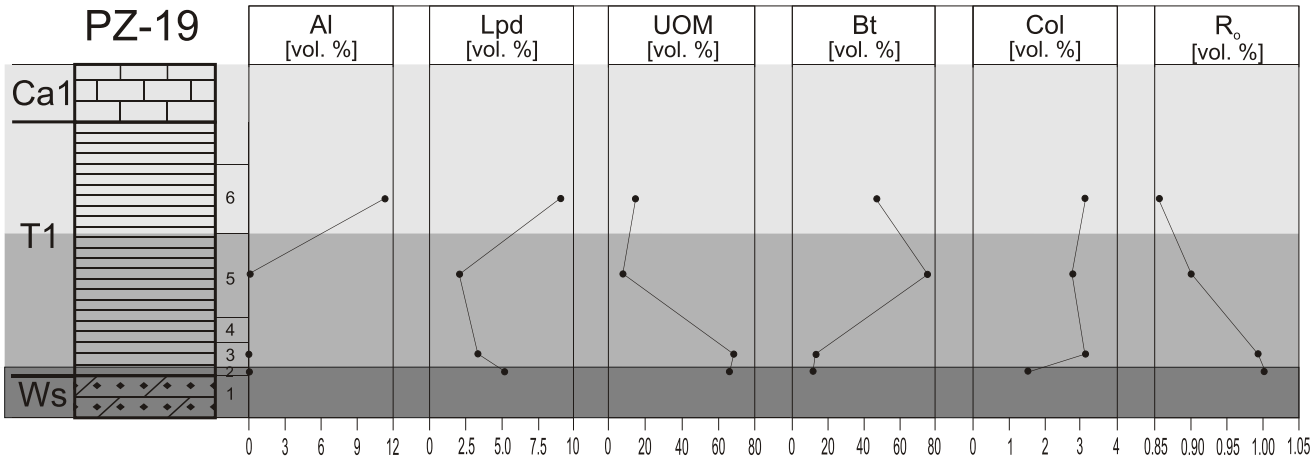

Fig. 5. Variation of maceral composition and vitrinite reflectance (R_o) of the Kupferschiefer shales of the PZ-19 section

Al — alginite, Lpd — liptodetrinite, UOM — unstructured organic matter, Bt — bituminite, Col — collinite

ORGANIC GEOCHEMISTRY

Kerogen was examined by the Rock-Eval pyrolysis. There is a gradual decline in the values of the S_1 and S_2 parameters and S_2/S_3 index toward the bottom of the profiles (Table 3). The hydrogen index (HI) reaches much higher values in reduced samples (196–276) than in oxidised and transitional samples (14–23), whereas the oxygen index (OI) and KTR show the opposing trend.

The extracted organic matter (EOM) comprises between 0.009 and 0.4% TOC, with the highest concentrations in the reduced rocks (Table 4). Consistent with the C_{org} and bitumen contents, the EOM values, normalised to organic carbon, varies from 40–56 mg/g C_{org} in the reduced samples, through 41–232 mg/g C_{org} in TZ, to 128–308 mg/g C_{org} in the oxidised samples (Fig. 7). The hydrocarbon content of the bitumen from the reduced samples varies from 36 to 59%, whereas it is more variable in TZ and oxidised samples (24–63% and 17–68%, respectively). The amount of saturated hydrocarbons is generally high in the reduced samples (34–53%) in comparison to the aromatic hydrocarbons (47–66%), whereas TZ and oxidised samples mostly have lower saturated hydrocarbon contents

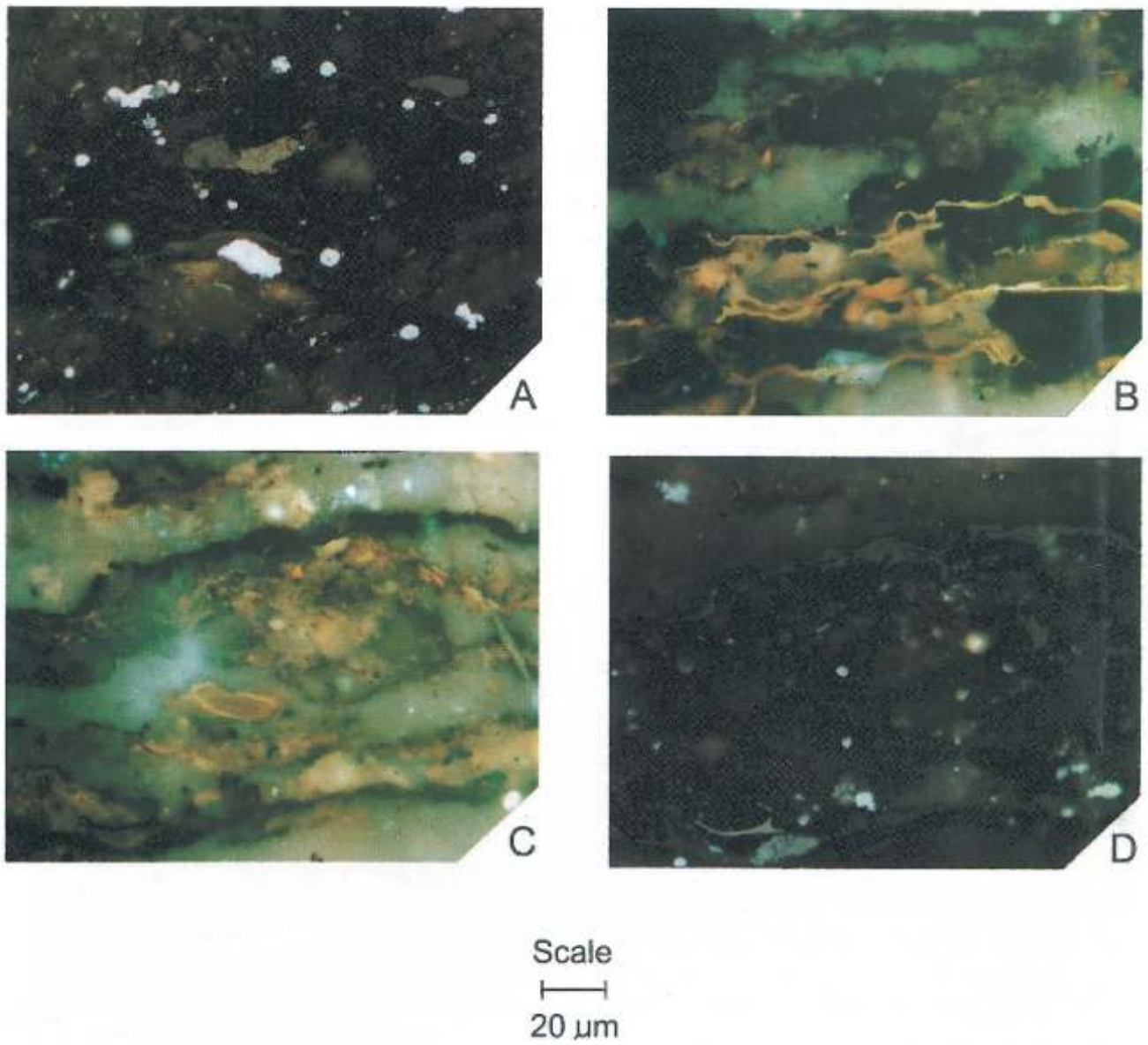

Fig. 6. **A —** vitrodetrinite and inertodetrinite (grey and light grey in colour, respectively) in the center, and thin band of vitrinite (grey) and the irregular band of vitrinite-like bituminite (dark grey) in the mineral background in the lower part of photo, reflected white light; **B —** thin elongated lamellae of lamalginite (dark yellow fluorescence colour), UV reflected light; **C** — an oval area of telalginite (weak fluorescence) surrounded by thin lammellae of lamalginite (strong fluorescence and intensive yellow colour) in the center, and vitrinite and a fragment of inertinite (black, non-fluorescent) below and above the telalginite/lamalginite composite, UV reflected light; **D —** plate Ic in fluorescence mode, UV reflected light

(5–22%). The previously known predominance of aromatic hydrocarbons in the oxidised rocks (Püttmann *et al.*, 1989; Bechtel *et al.*, 2000*a*) is illustrated by the Sat/Arom index (Fig. 7), the value of which is significantly lower in the oxidised rocks (0.1–0.3) than the reduced rocks (0.5–1.1).

The *n*-alkane and isoprenoid contents (Fig. 8) are generally higher in the reduced rocks (1.7–12.2 ppm *n*-alkanes, 0.38–1.55 ppm isoprenoids) than in the oxidised rocks (0.1–0.4 and 0.01–0.08 respectively) and correlate with the C_{org} contents (Oszczepalski, 1989; Püttmann *et al.*, 1989; Sawłowicz, 1989*a*; Bechtel *et al.*, 2000*a*). In the reduced rocks, a homologous, unimodal *n*-alkane envelope prevails displaying a harmonic decrease in *n*-alkane abundance with increasing carbon number. The *n*-alkane predominance in the range of low molecular weight within the reduced samples, with a maximum mostly at C_{17}, likely indicates a presumably large contribution of marine bacterial or algal input and a little higher plant input into the primarily marine algal/bacterial organic matter

Table 3

Rock-Eval pyrolysis data for the Kupferschiefer samples from the PZ-17 and PZ-19 sections

Section	Sample	Zone	TOC	T_{max}	S_1	S_2	S_3	S_2/S_3	KTR	HI	OI
			[wt.%]	[°C]	[mg HC/g rock]	[mg HC/g rock]	[mg CO_2/g rock]		$S_1/(S_1+S_2)$	[mg HC/g C_{org}]	[mg CO_2/g C_{org}]
PZ-17	5	r	8.44	438	1.94	23.37	0.69	33.87	0.08	276	8
	4	t	3.27	460	0.23	0.77	0.67	1.15	0.23	23	20
	2	o	0.39	I	0.02	0.07	0.31	0.23	0.25	17	79
PZ-19	6	r	6.06	435	1.22	11.93	0.68	17.54	0.09	196	11
	5	t	2.47	446	0.21	0.45	0.77	0.58	0.32	18	31
	4	t	3.91	466	0.23	0.56	1.49	0.38	0.29	14	38
	3	t	0.95	I	0.08	0.17	1.48	0.11	0.33	17	155
	2	o	0.20	I	0.07	0.11	-	-	-	-	-

For explanation see Materials and Methods; I — indeterminant due to low S_2 yield, related values are uncertain

(Gondek, 1980; Yawanarajah *et al.*, 1993), as detected by microscopy (Table 2). Most chromatograms of the oxidised and transitional samples are characterised by irregular, apparently bimodal or polymodal distribution patterns (Fig. 8). In these rocks, *n*-C_{17} — *n*-C_{20} alkanes predominate but there are smaller maxima in the range between *n*-C_{27} and *n*-C_{34}. This is also confirmed by the amounts of high molecular weight *n*-alkanes that are relatively high in the oxidised samples compared to short-chain *n*-alkanes, as shown by $\sum n$-C_{24+} (Fig. 8). In comparison to the reduced shales, the oxidised varieties are characterised by slight even-over-odd preference (CPI ≥ 1) and increased amounts of heavy odd-numbered *n*-alkanes vs. light odd-numbered *n*-alkanes (TAR ≥ 0.2). Enhanced percentage of even medium-chain *n*-alkanes (R22 > 1.2) in the oxidised rocks can be also noted.

The following polycyclic aromatic compounds (PAH): biphenyl, dibenzofuran, phenanthrene, methylphenanthrenes, fluoranthene, pyrene, chrysene and the polyaromatic sulfur hydrocarbon (PASH) — dibenzothiophene were identified (Table 5, Fig. 9). The total amounts of identified PAHs and the phenanthrene/methylphenanthrenes index (Ph/MPh) values are highest in the transitional samples. Earlier determinations on the S-2 samples (Oszczepalski and Otwinowska, unpubl.) also established higher Ph/MPh values (> 3.1) in TZ zone vs. reduced and completely oxidised samples. The Fla/Pyr ratio and the distribution of dibenzothiophene and chrysene parallel the

Table 4

Organic geochemical data for the Kupferschiefer samples from the S-2, PZ-17 and PZ-19 sections

Section	Sample	Zone	C_{org}	EOM		HC	Sat		Arom		Sat/Arom	Res	Asph	Sat+Arom/ Res+Asph
			[%]	[ppm]	[mg/g C_{org}]	[% EOM]	[% HC]	[% EOM]	[% HC]	[% EOM]		[% EOM]	[% EOM]	
S-2	51	r	2.06	1042	50.6	47.0	48.9	23	51.1	24	1.0	-	-	1.0
	53	r	2.14	1193	55.7	59.0	42.4	25	57.6	34	0.7	-	-	0.7
	55	r	3.64	1470	40.4	50.0	34.0	17	66.0	33	0.5	-	-	0.5
	57	r	3.25	1646	50.6	36.0	52.8	19	47.2	17	1.1	-	-	1.1
	58	t	0.30	695	231.7	63.0	14.3	9	85.7	54	0.2	-	-	0.2
	60	t	0.30	514	171.3	56.0	17.9	10	82.1	46	0.2	-	-	0.2
	62	o	0.29	893	307.9	68.0	11.8	8	88.2	60	0.1	-	-	0.1
PZ-17	5	r	7.15	4020	56.2	40.7	46.5	19	53.5	22	0.9	7	52	0.9
	4	t	2.19	1210	55.3	36.1	12.0	4	88.0	32	0.1	2	62	0.1
	2	o	0.52	260	50.0	27.4	21.9	7	78.1	25	0.3	2	66	0.3
	1	o	0.06	120	200.0	-	-	-	-	-	-	-	-	-
PZ-19	6	r	4.46	2430	54.5	42.4	49.0	21	51.0	22	1.0	8	49	1.0
	4	t	3.33	1820	54.7	24.4	8.4	2	91.6	22	0.1	-	-	0.1
	3	t	0.91	380	41.8	34.0	5.7	2	94.3	32	0.1	-	-	0.1
	2	o	0.07	90	128.6	17.3	-	-	-	-	-	-	-	-

EOM — extracted organic matter, HC — hydrocarbons, Sat — saturated hydrocarbons, Arom — aromatic hydrocarbons; Res — resins; Asph — asphaltenes

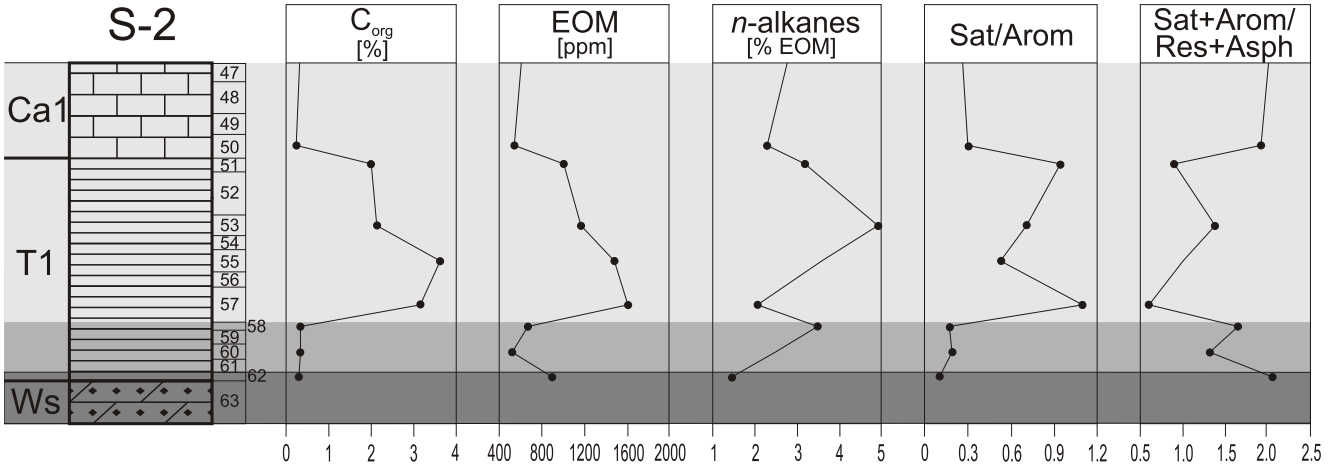

Fig. 7. Variation of C_{org}, EOM, *n*-alkanes, Sat/Arom index and Sat+Arom/Res+Asph index in the S-2 section

Ph/MPh ratios, whereas the fluoranthene and pyrene percentages gradually increase towards the oxidised rocks. The methylphenantrene index MPI-1 values generally decline downwards but are lowest within the TZ.

In the case of heterocompounds, resins and asphaltenes make up 41–64% of the bitumen in the reduced samples and 32–69% in the oxidised and transitional samples (Table 4, Fig. 7). The resins content in bitumen of the reduced rocks (6–9%) is higher than in the oxidised rocks (2–3%). The inverse trend is characteristic for the asphaltene content — 61–66% in the oxidised rocks, 49–53% in the reduced.

ISOTOPE STUDIES

C isotopes in the organic matter. The $\delta^{13}C$ (PDB) analyses yield a narrow range from –27.9 to –26.6‰ (Table 6) in accordance with isotope data for Permian age organic substance. Both the Rote Fäule and Cu-mineralised rocks display heavier $\delta^{13}C$ values for kerogen than the barren Kupferschiefer; –27.0 to –20.1‰ for the Richelsdorf deposit (Bechtel and Püttmann, 1991), –27 to –22‰ for the Konrad mine (Püttmann *et al.*, 1993), and –28.2 to –24.4‰ for numerous localities throughout the Polish basin (Bechtel *et al.*, 2000*a*). In the profiles studied, this pattern was less clear (Table 6). The isotopic composition of carbon in the kerogen of the reduced samples varies to a small degree, typical for organic material of algal and bacterial origin, with an insignificant land plant material contribution. This degree of variation is characteristic for kerogen type II representing marine organic matter (Galimov, 1980).

The bitumen is characterised by variable C isotope ratios similar to those for kerogen, although it shows slight ^{13}C depletion relative to kerogen (Table 6). Note that TZ bitumen (similarly to the kerogen and aromatic hydrocarbons) is slightly enriched in light ^{12}C isotope vs. the rest of the sections studied. Furthermore, in the heterocompounds it is possible to observe a gradual increase in the content of this isotope towards the oxidised rocks. The reverse is true for saturated hydrocarbons; the oxidised rocks are characterised by a fall in heavy isotope content compared to the reduced samples.

From the $\delta^{13}C$ ratios for the saturated and aromatic hydrocarbons (*cf.* Sofer, 1984) it emerges that the precursors of the bitumen were cyanobacteria and algae. The C isotope composition of the bitumen, in its particular fractions and in the kerogen (Table 6), is evidence of the examined organic matter presumably having come from one source, and that the bitumen and kerogen are indigenous. The impoverishment of the bitumen in ^{13}C isotope relative to kerogen is apparently a result of the enrichment of the saturated hydrocarbons in the light carbon isotope, as the hydrocarbons accumulated in the sediment due to the diagenesis of organic material (Galimov, 1980). It can be seen from the $\delta^{13}C$ of the saturated and aromatic hydrocarbons that the amount of algal-type material decreased relative to the amount of terrigenous material in the oxidised samples (Table 6).

C and O isotopes in the carbonates. $\delta^{13}C$ (PDB) data from the Kupferschiefer carbonates varies between –2.1 and 3.5‰ and $\delta^{18}O$ (PDB) between –8.4 and 0.4‰ (Table 6). There is a clear tendency towards an enrichment of the transitional and oxidised zone in the light isotopes of carbon and oxygen relative to the rest of the sections. Oxidised samples are characterised by $\delta^{13}C$ of –0.8 to 0.9‰ and $\delta^{18}O$ of –8.4 to 0.4‰, TZ samples by $\delta^{13}C$ of –2.1 to 0.4‰ and $\delta^{18}O$ of –4.1 to 0.1‰, as opposed to reduced samples that have $\delta^{13}C$ from 0.9 to 3.5‰ and $\delta^{18}O$ from –0.8 to 1.8‰. Sawłowicz (1989*b*) obtained comparable results for the slightly oxidised rocks of the Lubin-Sieroszowice deposit ($\delta^{13}C$ –0.9 to 0.0‰, $\delta^{18}O$ –12.3 to –7.4‰). Similar records for the Rote Fäule were presented by Hammer *et al.* (1990) for the Mansfeld-Sangerhausen deposit

($\delta^{13}C$ –5.0 to –2.2‰, $\delta^{18}O$ –10.1 to –4.9‰), and Bechtel and Püttmann, (1991) for the Richelsdorf deposit ($\delta^{13}C$ –4.4 to –2.5‰, $\delta^{18}O$ –12.3 to –9.7‰). The $\delta^{13}C$ in the reduced rocks of the Lubin-Sieroszowice deposit ranges from –0.2 to 4.3‰ and $\delta^{18}O$ from –16.8 to 0.9‰ (Sawłowicz, 1989*b*; Bechtel *et al.*, 2000*a*), similarly to the Richelsdorf deposit (–3.2 to 2.9‰ and –9.3 to –3.4‰ respectively). Slightly different data ranges and trends for these isotopes with a tendency towards an increase in the content of the heavy carbon and oxygen were found for locations distant from the oxidised zone. They are reported from the Pb-Zn zone of the Lubin-Sieroszowice deposit ($\delta^{13}C$ of the order of 2 to 4‰ and $\delta^{18}O$ in the range –10 to 3‰; Harańczyk, 1986), the Richelsdorf deposit ($\delta^{13}C$ from –1.0 to 2.7‰ and $\delta^{18}O$ from –9.0 to –4.2‰; Bechtel and Püttmann, 1991), the Mansfeld-Sangerhausen deposit ($\delta^{13}C$ from –2.7 to 1.7‰ and $\delta^{18}O$ from –9.5 to 3.7‰; Hammer *et al.*, 1990), and from the barren, pyritiferous shales ($\delta^{13}C$ between 1 and 4‰ and $\delta^{18}O$ from –5 to –1‰; Vaughan *et al.*, 1989; Bechtel *et al.*, 2000*a*).

O isotopes in the sulfates. Sulfates finely disseminated through the shales have $\delta^{18}O$ values ranging from –1.4 to 11.8‰ (SMOW). While most sulfates yielded $\delta^{18}O$ data in the range between 8.8 and 11.8‰, similar to those of Permian marine sulfates, the reduced shales directly overlying TZ have distinctly lower $\delta^{18}O$ values covering a range from –1.4 to –0.9‰ (Table 6).

S isotopes in the sulfides and sulfates. The $\delta^{34}S$ (CDT) records from the disseminated sulfides exhibit a rather large range of values, from –41.4 to –15.3‰, depending on the redox of host rocks (Table 6). In the reduced rocks the sulfide sulfur is remarkably enriched in light sulfur ^{32}S ($\delta^{34}S$ from –41.4 to –33.7‰), whereas the oxidised rocks contain significantly more heavy sulfur ^{34}S ($\delta^{34}S$ from –33.3 to –15.3‰). The $\delta^{34}S$ value of the pyrite varies in a broad range from –52 to –25‰ (Marowsky, 1969; Vaughan *et al.*, 1989; Jowett *et al.*, 1991*a*), with a rough average of –35‰ (Harańczyk, 1986). Considering the lack of pyrite in the basal part of the reduced samples studied (Fig. 4), it should be assumed that the fine-grained copper sulfides have sulfur fractionation in the range –40 to –33‰, similar to the previous values (–40 to –26‰) from various localities of the Lubin-Sieroszowice deposit (Harańczyk, 1986; Sawłowicz, 1989*b*; Jowett *et al.*, 1991*b*). A very similar $\delta^{34}S$ range from –36 to –31‰ was also obtained for base-metal sulfides in the North Sudetic Trough and Central Poland (Jowett *et al.*, 1991*a*, *b*). Taking all results into account along with the results of their study, Wodzicki and Piestrzyński (1994) give an average $\delta^{34}S$ value of –34.8‰ from the disseminated ores.

The analysis of sulfur isotopes in the sulfates was done separately for late-diagenetic anhydrite nodules and the sulfates dispersed through the rock (Table 6). The nodules have $\delta^{34}S$ (CDT) ranging from 7 to 12‰. The fractionation of the sulfur isotopes in the dispersed sulfates varies to a great degree, from –25.0 to 7.6‰ (CDT), where the maximum light sulfur enrichment ($\delta^{34}S$ from –25.0 to –2.8‰) was found at the base of the reduced zone (S-2 section) and at the top of the transition zone (PZ-19 section).

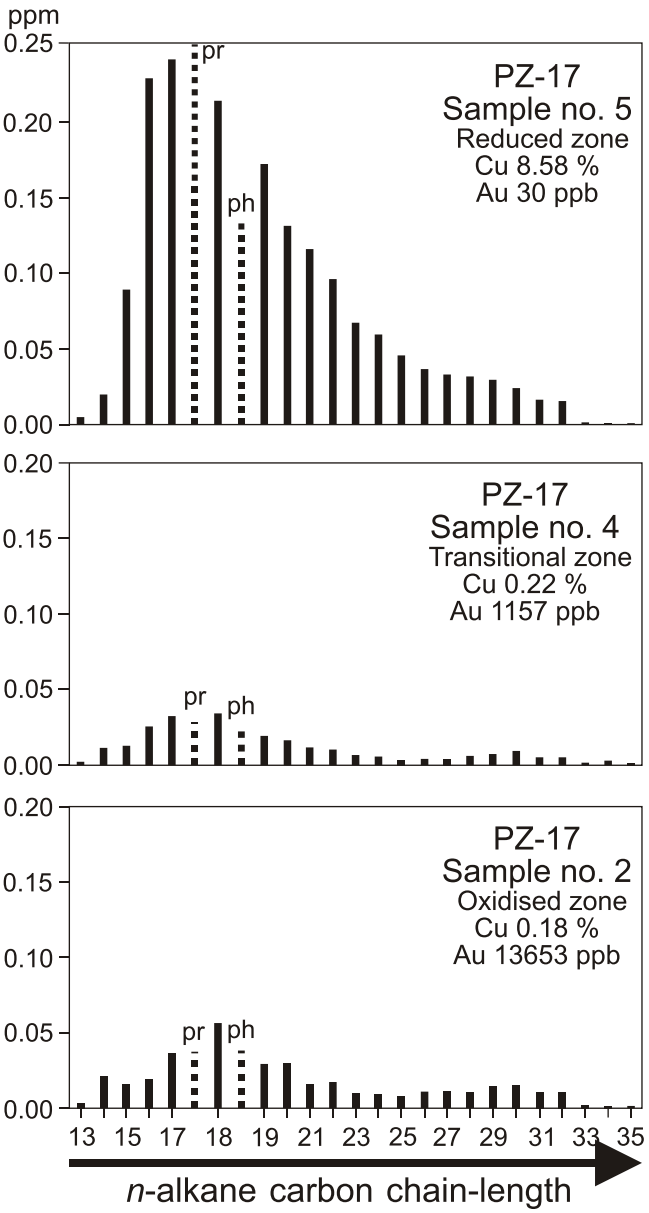

Fig. 8. Representative *n*-alkane and isoprenoid (pr — pristane, ph — phytane) distributions for the saturated hydrocarbon fraction of the three extracts from the PZ-17 section

DISCUSSION AND IMPLICATIONS

METAL REDISTRIBUTION ACROSS AN OXIDATION FRONT

Integration of bulk chemical data provides evidence that geochemical parameters are useful in indicating the post-depositional alteration and significant redistribution associated with the progressed redox front. The downward increase in potassium content, illustrated by the K_2O/Na_2O ratio (Table 1) indicate potassic diagenesis, which caused the recrystallisation of illite and/or its neoformation in the oxidised

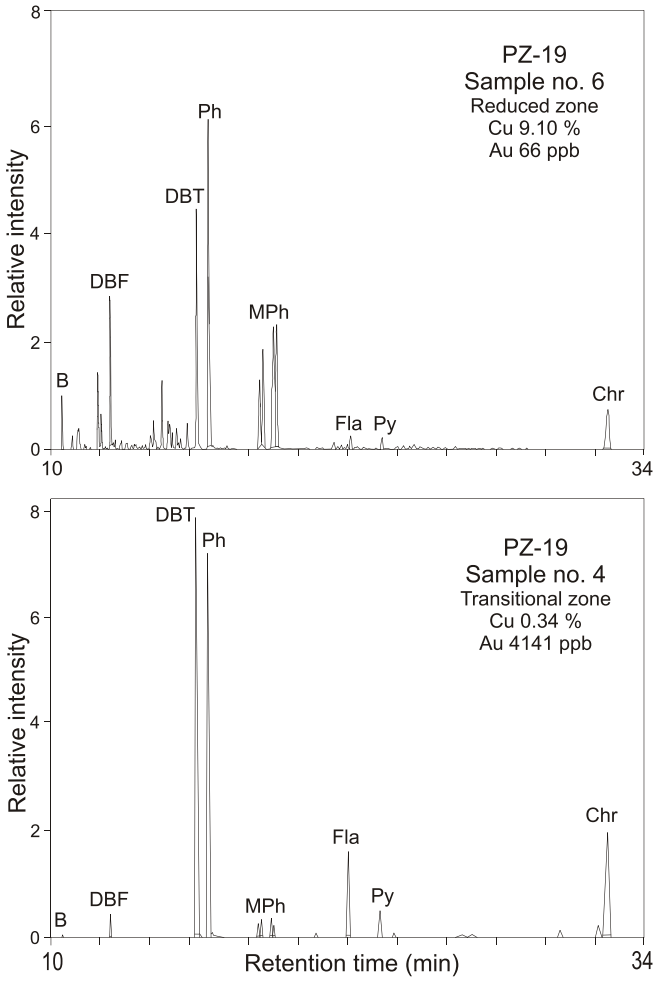

Fig. 9. Representative gas chromatograms showing the distribution of aromatic hydrocarbons separated from the total extract of two selected Kupferschiefer samples, PZ-17 section

B — biphenyl, DBF — dibenzofuran, DBT — dibenzothiophene, Ph — phenanthrene, MPh — methylphenanthrene, Fla — fluoranthene, Py — pyrene, Chr — chrysene

and ore-bearing rocks (Bechtel *et al.*, 2000*b*). The parallel trend in MgO/CaO ratio might be explained by the enhanced calcitisation of the oxidised rocks by Ca^{2+}-rich waters (Oszczepalski, 1989; Kucha and Przybyłowicz, 1999). The association of the highest Cu, Ag, Pb, Zn, Co, Mo, Ni, and Ta concentrations with the reduced facies is a characteristic feature of Zechstein mineralisation, although the sections studied, located at the transition from Rote Fäule to the Cu zone (Fig. 1) are poor in Pb and Zn. All of these metals are related to the C_{org} and reduced sulfur contents (Table 1). A positive correlation is known to exist between the C_{org}, Ag, Cu and S^{2-} contents for the mineralised shales (Harańczyk, 1986). The Cr concentration, dependent mostly on the presence of terrigenous material, has a pattern independent of mineralisation processes. As a result, the V/Cr index (*cf.* Sun and Püttmann, 1997), like the increased Au, Pt, Pd, and locally U and Hg contents (Table 1, Fig. 3), may serve as a parameter distinctive for the TZ. Because a significant amount of the Ni (unlike Co) is concentrated in the sediment mainly as a result of absorption by clay-organic material, low Co/Ni ratio values are characteristic of the oxidised rocks. The concentrations of Re and Ir are highest in the reduced shales, whereas the concentrations of Se and REE are highest in oxidised samples (Hammer *et al.*, 1990; Kucha and Przybyłowicz, 1999; Bechtel *et al.*, 2001*b*). The positive Sm anomalies and negative Ce and Eu anomalies within the uppermost part of the oxidised interval imply redistribution of REE during formation of the Rote Fäule (Kucha and Przybyłowicz, 1999; Bechtel *et al.*, 2001*a*).

These data collectively suggest that the Kupferschiefer shales have been strongly altered. The observed metal distribution and a rise in Fe^{3+}, K_2O, CaO (locally) contents and fall in C_{org}, S_{tot}, S^{2-} towards the base of the profile (Table 1) indicates a downward increasing oxidation effect and argues for an upward movement of the oxidising fluids. This is also demonstrated by the textural and paragenetic relationships along the profiles studied (Fig. 4). Numerous hematitic spherules pseudomorphic after framboidal pyrite typically occur within the oxidised rocks. The pyrite content of unoxidised Kupferschiefer is typically 2–3 vol.% (Oszczepalski and Rydzewski, 1991), but at the base of the reduced shales it drops rapidly and in the oxidised zone it diminishes to essentially all hematite (Fig. 4). Numerous replacements of copper sulfides with hematite and goethite were also found in the Rote Fäule (Rydzewski, 1978; Oszczepalski, 1994, 1999). Oxidation of pyrite would have released sulfates and created initial acidity of the fluid, which enhanced leaching of metals, dissolution and calcitisation of oxidised carbonates. Interaction of the mineralising fluids with the host rocks caused the Eh fall as the fluids progressively migrated into the Kupferschiefer and deposited metals according to their decreased solubility. The cross redox metal zoning from the lower parts of the oxidised hematitic zone to the reduced pyritiferous rocks: Fe^{3+}-Fe^{3+}, Au, Pt, Pd-Cu, Ag-Cu, Pb, Zn, Fe^{2+}-Fe^{2+} is consistent with the interaction of the oxidising fluid passage from underlying Rotliegend aquifer (Jowett, 1986; Oszczepalski and Rydzewski, 1997; Bechtel *et al.*, 2001*a*). Remnants of copper sulfides in the oxidised shales imply that copper, silver and associate metals were carried away from the sediments, which underwent oxidation, and were deposited within the organic carbon-rich shales. Furthermore, detailed work has shown that the Rote Fäule/ore system cuts across the strata having features indicating post-depositional origin (Rydzewski, 1978; Oszczepalski 1989).

As indicated above, the TZ has intermediate features relative to oxidised and reduced rocks, indicating that in this transition, complex water-rock interactions occurred. A combination of alternating oxidation, acidification, and successive processes of neutralisation, moderate reduction and sulfide precipitation induced sulfide oxidation, leaching and fixation of base and precious metals. Pronounced enrichment of PGE, REE, V, U, Se, and Hg within the topmost part of the TZ and the occurrence of base metal ores at the reduced side of the redox interface argues for efficient metal redistribution during formation and expansion of the Rote Fäule. As in most of the base metals, precious metals were preferentially transported as chloride complexes ($AuCl^{4-}$, $PtCl_4^{2-}$, $PtCl_6^{2-}$, $PdCl_4^{2-}$), which are typical species in chloride-rich but sulphide-poor solutions

Table 5

Relative proportions of selected aromatic hydrocarbons and related indices for the Kupferschiefer samples from the PZ-17 and PZ-19 sections

Section	Sample	Zone	PAH	B	DBF	DBT	Ph	3MPh	2MPh	9MPh	1MPh	Fla	Py	Chr	Ph/MPh	MPI-1	Fla/Pyr
			[ppm]	[%]													
PZ-17	5	r	0.8	0.1	0.6	11.1	19.5	4.2	4.8	9.8	6.6	2.1	2.0	39.2	0.8	0.4	1.0
	4	t	3.5	0.2	2.3	13.7	17.3	1.0	1.3	2.2	1.4	4.5	1.5	54.6	2.9	0.2	3.0
	2	o	1.9	0.1	0.1	5.2	10.4	0.8	1.2	1.9	1.3	7.0	2.5	69.5	2.0	0.2	2.8
PZ-19	6	r	2.4	1.6	4.3	12.1	25.1	4.6	5.6	11.0	7.9	1.2	1.3	25.3	0.9	0.4	0.9
	4	t	3.4	0.1	0.4	16.9	18.9	0.5	0.6	0.7	0.4	6.8	2.1	52.6	8.6	0.1	3.2
	3	t	1.3	0.5	3.1	18.9	20.5	0.4	0.4	0.6	0.3	6.6	2.0	46.7	12.1	0.1	3.3
	2	o	0.1	0.0	1.8	1.9	14.8	1.8	1.8	1.9	1.8	33.3	13.0	27.9	2.0	0.3	2.6

PAH — total identified polycyclic aromatic hydrocarbons in aromatic hydrocarbons; Ph/MPh — phenanthrene/methylphenanthrenes, MPI-1 = 1.5 (MPh-2 + MPh-3)/Ph + MPh-1 + MPh-9

(Romberger, 1988; Wood *et al.*, 1992; Gammons, 1995). Thermodynamic calculations and experimental data indicate that saline fluids in equilibrium with hematite are capable of transporting significant quantities of gold and PGE (Jaireth, 1992; Wood *et al.*, 1992). These chloro-complexes might have been alternately reduced and sorbed by organic matter and pyrite (e.g. Hyland and Bancroft, 1990; Jaireth, 1992; Mycroft *et al.*, 1995) and adsorbed by iron oxides (e.g. Machesky *et al.*, 1991). Gold and PGM were also coprecipitated with copper sulfides, as evidenced by relict parageneses found at the oxidised side of the redox front and fairly common intergrowths of gold and copper sulfides and Pd arsenides within reduced rocks adjacent to the Rote Fäule (Kucha, 1981; Piestrzyński *et al.*, 1997; Kucha and Przybyłowicz, 1999). Characteristically, the enrichments in precious metals correspond with the enhanced occurrence of solid bitumen within the oxidised rocks (*cf.* Table 1 and 2). Hence, oxidising fluids could have influenced deposition of solid bitumen that in turn could promote incorporation of precious metals. More study is required to explain this association; nevertheless, Au found to be fixed by thucholite (Kucha, 1981) suggests that it is prudent to consider solid bitumens as the residence of the precious metals. Thiosulfate ions ($S_2O_3^{2-}$) and other intermediate sulfoxy species, being products of sulfide oxidation (Goldhaber, 1983; Wood *et al*. 1992), might have played a considerable role in the redistribution of base- and precious metals within the oxidised rocks (Kucha, 1990; Piestrzyński and Wodzicki, 2000). As a result, the least mobile metals such as PGM concentrated in the oxidised rocks, whereas the more soluble base metals were advanced to the less oxidised and reduced Kupferschiefer varieties, as the redox front migrated higher from the Rote Fäule. Both replacements of sulfides by iron oxides, intergrowths of Au, Pt and Pd minerals, and overgrowths of the gold by hematite, indicate that hematisation overlapped with deposition of early pyrite and copper ores and post-dated the precipitation of gold. Alternatively, Kucha and Przybyłowicz (1999) suggested that the precious metals could have been introduced after Cu emplacement.

ALTERATION OF ORGANIC CONSTITUENTS

Previous maceral studies in the Lubin-Sieroszowice region were performed solely on the reduced shales (Rospondek *et al.*, 1993; Sun *et al.*, 1995). This study provides organic petrology data also for the oxidised sections, showing trends in composition (Fig. 5), which are interpreted to indicate that most of the organic components are sensitive to alteration. Note that the most labile components of marine and terrestrial origin (alginite and collinite, respectively) are present almost exclusively in the reduced rocks, and in the oxidised rocks are only a trace component. It was shown that the oxidised rocks do not differ from the reduced variety in terms of their depositional features, indicating formation in a similar anaerobic-to-dysaerobic sedimentary setting (Oszczepalski, 1989). Thus, the maceral composition in the oxidised rocks seems to be a result of post-sedimentary oxidative degradation of labile components and the diagenetic transformation of the macerals into refractory forms resistant to further changes. This is clearly shown by a gradual increase in the alginite, bituminite, collinite and sporinite content, and a decrease in the solid bitumen content upwards to the reduced horizon, and corresponds to the previous results obtained in the Konrad (Speczik and Püttmann, 1987; Speczik, 1994) and Polkowice profiles (Sun, 1998).

The reduced samples predominantly contain primary material of marine origin, especially alginite — the diagnostic maceral for the reduced shales. Liptodetrinite, sporinite and terrigenous collinite, derived possibly from coalification of amorphous humic matter, are also abundant. On a contrary, the oxidised sediments contain mainly UOM, followed by bituminite, liptodetrinite and vitrinite (Table 2). Thin liptinite and collinite laminae, oriented always parallel to stratification imply that primary organic matter was originally present in the oxidised rocks in presumably greater amounts. The co-occurrence of relict organic constituents with iron oxides replacing pyrite and copper sulfides within the oxidised lithologies strongly suggests that organic matter was also largely changed by oxidation. Therefore, bituminite, abundant mostly in the upper part of the oxidised sequence (TZ) as thin laminae, is considered to be a product of oxidative alteration of lamalginite. Fairly small amounts of liptinite macerals and the absence of alginite and sporinite support this. More evidence of the downhole increase in oxidation intensity is the trace content in the oxidised rocks of terrigenous sporinite, which is resistant to degradation.

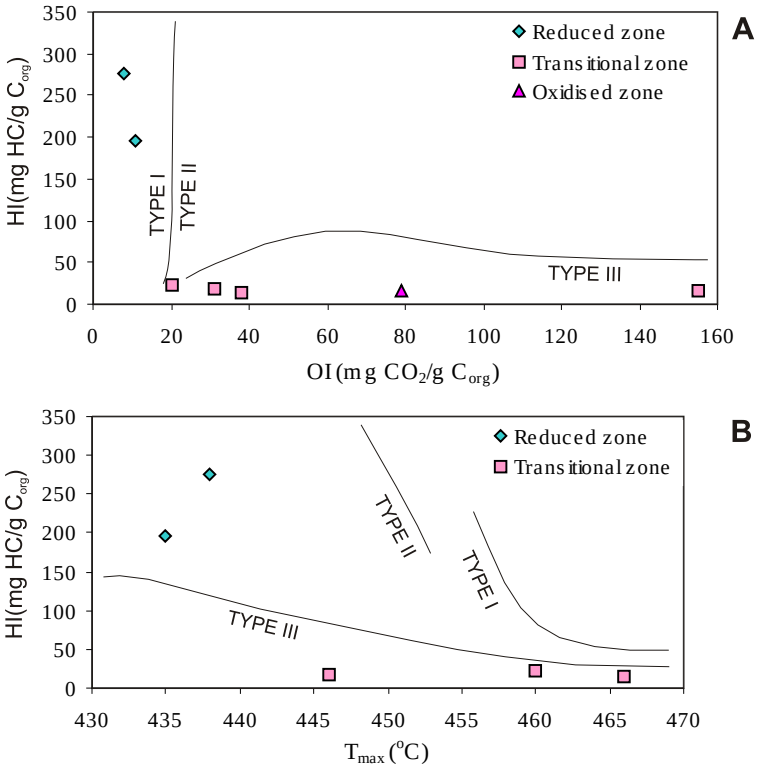

Fig. 10. Rock-Eval pyrolysis results for Kupferschiefer samples from the S-2, PZ-17, and PZ-19 sections (kerogen types after Espitalie *et al.*, 1977); A — hydrogen index vs. oxygen index diagram, B — hydrogen index vs. T_{max} diagram

UOM occurs predominantly in the oxidised shales mostly as solid bitumen making up 65–92% of the microscopically observed constituents. Only relicts of copper sulfides and primary organic matter and an abundance of solid bitumen characterise the oxidised shales, whereas alginite, sporinite and AOM are almost absent. A possible explanation for an increase in solid bitumen is its generation at the expense of liptinite and vitrinite macerals, as a result of water washing, biodegradation, deasphalting, sulphate reduction or radiolysis (*cf.* Curiale, 1986; Jacob, 1989; Landis and Castano, 1994; Machel *et al.*, 1995), taking place due to the action of the oxidising fluids. Kucha and Przybyłowicz (1999) postulated a radiolysis of hydrocarbons by uranium as a powerful agent, enhancing oxidation of organic matter and solidification of bitumen. As a consequence of these processes, the alteration further caused an increase in reflectance of non-recycled vitrinite towards the bottom of the Kupferschiefer, from 0.72–0.86% in the reduced rocks, through 0.72–1.13% in the TZ, to 1.03–1.10% in the oxidised rocks (Fig. 5). This variation is consistent with previous observations (Speczik and Püttmann, 1987; Sun, 1998). The increased reflectance of the indigenous organic matter seems to be a function of the intensity of ascendant circulation of oxidising fluids. Refractory, corroded vitrodetrinite macerals having high reflectance, and oxidation rims indicate that they are recycled ("allochthonous") organic particles, redeposited from the Zechstein footwall. Hence, their formation is not related to the formation of Rote Fäule.

The low concentration of highly inert terrestrial particles in the form of inertodetrinite, both in reduced and oxidised samples, is remarkable (Table 2). Such a low inertinite content is typical of anoxic environments, distant from the coast. Assuming vitrinite, sporinite and inertinite to be terrigenous, the total land-derived components vary between 6 and 19%, despite the oxidised or reduced character of the host rocks. Taking into account these results it can be assumed that the high amount of inertinite identified at the base of the Konrad profile, interpreted as a result of vitrinite oxidation (Sun *et al.*, 1995), reflects the influx of terrigenous detritus from the coast.

OXIDATION-INDUCED COMPOSITIONAL CHANGES IN KEROGEN AND BITUMEN

Geochemical changes were observed with depth indicating that the lowermost portions of the Kupferschiefer sections underwent severe chemical alteration. The mean vitrinite reflectance values (ranging between 0.7 and 1.2%) correspond to the oil window, indicating that bitumens were generated at the catagenetic stage of kerogen maturation. Low K values (C21 + C22/C28 + C29) and high values of TAR (C27 + C29 + C31/C15 + C17 + C19) and $\sum n\text{-}C_{24+}$ indices, characteristic of the oxidised samples, suggest a larger terrestrial contribution to TOC (*cf.* Tissot and Welte, 1984). However, these degraded distribution signatures in transitional and oxidised samples (Fig. 7) indicate rather that low-to-medium molecular weight

n-alkanes were preferentially removed from the system as a result of advanced decomposition of the labile components of algal and bacterial origin (Bechtel *et al.*, 2000*a*). It has been shown that light *n*-alkanes are effectively biodegraded and decomposed by oxidation (e.g. Ezra *et al.*, 2000). This process might have been accompanied by a selective removal of the light odd-numbered *n*-alkanes, as might be suggested from the characteristics of residual bitumen in the oxidised rocks, showing relative enrichment in long chain *n*-alkanes and a slight EOP preference. Large variations in pr/ph and isoprenoid/alkane ratios may reflect different degradation and maturity constraints assuming similar primary organic matter. Thus, biomarker composition, changing independently of maturity parameters indicates that distribution of biomarkers was influenced by oxidation.

In contrast to the reduced shales, the oxidised samples are enriched in high molecular weight unsubstituted PAHs (fluoranthene, pyrene, chrysene), which are resistant to degradation (e.g. Ezra *et al.*, 2000), and depleted in alkylated phenanthrenes (methylphenanthenes) by about 75% relative to the reduced lithologies (Table 5, Fig. 9) that argues for a post-depositional removal from these rocks. The Ph/MPh index was used to define the intensity of the oxidation process (Speczik and Püttmann, 1987; Püttmann *et al.*, 1989, 1991; Sun, 1998; Bechtel *et al.*, 2000*a*, 2001*b*). As evidenced by previous and present data, the higher Ph/MPh ratios (> 1) point to increased oxidation and might be interpreted as a result of late-diagenetic decomposition of alkylated aromatic hydrocarbons by oxidising fluids. As considered by Püttmann *et al.* (1991), hydrothermal solutions could add some PAHs and PASHs derived from gas generated in Carboniferous strata. This might argue for a concomitant transport of the PAHs and the precious metals in ascending oxidising solutions, and a contribution of metal-organic complexes in mobilisation and transport of gold (Bechtel *et al.*, 2001*a*). However, gradual content variability of many of PAHs along the profiles studied (Table 5) and preferential accumulation of phenanthrene and PASHs in the TZ may rather be explained by *in situ* desalkylation.

HI/OI and HI/T_{max} diagrams, comparable to modified van Krevelen diagrams (Espitalie *et al.*, 1985), clearly demonstrate that the reduced and oxidised samples occupy different fields in the scatter plots (Fig. 10). The results are in accordance with previous Rock-Eval data obtained for the Konrad mine (Püttmann *et al.*, 1991; Sun *et al.*, 1995). The oxidised samples contain a terrigenous type III kerogen, which is occasionally considered to be residual (type IV) kerogen, due to its very low H/C value, indicative of the presence of oxidised, largely inert terrigenous organic matter. The very low S_2/S_3 index value (< 1.2) is evidence of a lack of sapropelic admixtures in the kerogen, thus indicating that the oxidised samples are extremely depleted in hydrogen. The temperatures of maximum pyrolysis (T_{max}) yield range from 435 (reduced shales) to 466°C (oxidised shales). Although the credibility of T_{max} measurements for rocks depleted in C_{org} may be questioned, nevertheless T_{max} values seem to be in harmony with the other maturity parameters. High T_{max} values and the KTR index (Table 3) indicate the kerogen from the oxidised samples to be mature with regard to oil generation.

Unlike the oxidised rocks, the reduced shales contain mixed hydrocarbon-prone type II kerogen enriched in hydrogen-rich liptinites (Figs. 5 and 10), which represents material derived from a mixture of phytoplankton and bacteria biomass, capable of generating hydrocarbons (Teichmüller and Durand, 1983). The definite prevalence of sapropelic material over humic matter is confirmed by the high S_2/S_3 index values (17–34). The T_{max} temperature value (435–438°C), the presence of free hydrocarbons (S_1 in the range 1.22–1.94 mg HC/g of rock) and the low KTR index value (about 0.09) coupled with a relatively low R_o (0.7–0.9) suggest that the reduced sediments entered the catagenesis stage (50–150°C) of oil generation, but they have not generated much oil. The generation potential of the reduced source rock is still not exhausted, as suggested by the high S_2 parameter value (11.93–23.37 mg HC/g rock). The low OI values (in the range 8–11 mg CO_2/g TOC) are evidence that the kerogen in the reduced rocks was not subjected to oxidation.

Finally, the downhole increase in the T_{max} value (Table 3) agrees with reflectance results (Table 2). The systematic decrease in C_{org} and HI values from the top to the bottom of the examined profiles, corresponding to the increasing maturity of the kerogen, the increasing hematite content and the increasingly intensive features of maceral and sulfide oxidation, indicates a post-sedimentary degradation of organic material related to the formation of the Rote Fäule. This pattern cannot be explained by variability in the redox conditions of the depositional environment, as, from sedimentary investigations it is known that in the Lubin-Sieroszowice region, the most reducing depositional conditions existed at the start of the Kupferschiefer sedimentation (Oszczepalski, 1989; Sawłowicz, 1989*a*; Rospondek *et al.*, 1994; Sun *et al.*, 1995). Thermal maturity variations, due to the short time the Kupferschiefer was deposited in and its very slight thickness, also cannot explain this variability. This trend rather is thought to indicate that the downward increase in alteration intensity is an effect of secondary degradation of organic matter by incoming oxidising solutions after partial diagenetic maturation of the organics, as previously suggested in numerous studies (Speczik and Püttmann, 1987; Bechtel and Püttmann, 1991; Püttmann *et al.*, 1989, 1991; Sun and Püttmann, 1997; Kucha and Przybyłowicz 1999; Bechtel *et al.*, 2000*a*, 2001*b*). The dependence of HI on C_{org} values (Tables 3 and 4) shows that only the reduced samples have a positive correlation. Thus, as in the case of the Konrad profile, the oxidation processes are thought to cause the preferential destruction of the aliphatic hydrocarbons, the alteration of bitumen into an aromatic-asphaltic type, and the transformation of bitumen into the form of solid bitumen. As a result, strongly degraded hydrogen-poor and aromatic-rich kerogen formed in the oxidised rocks, lacking to a significant extent its syngenetic components (Fig. 10). Assuming that the oxidised shales primarily contained similar amounts of C_{org} and S_{tot} as the equivalent reduced varieties, it is evident from these data that more than 90% C_{org} and S_{tot} and more than 80% of bitumen were removed from the lowermost portions of the Kupferschiefer during post-sedimentary oxidation. Water washing, biodegradation, oxidation, and radiolysis have been quoted as the principal processes responsible for the removal of bitumen and alteration of organic matter (Tissot and

Table 6

Carbon, oxygen and sulfur isotopic composition (in ‰) of organic matter, carbonates, sulfides, disseminated sulfates, and nodular sulfates in the S-2, PZ-17 and PZ-19 Kupferschiefer sections

Section	Sample	Lithostr	Zone	$\delta^{13}C$ [PDB]							$\delta^{18}O$ [PDB]	$\delta^{18}O$ [SMOW]	$\delta^{18}O$ [SMOW]	$\delta^{34}S$ [CDT]	$\delta^{34}S$ [CDT]	$\delta^{34}S$ [CDT]
				Ker	Bit	Sat	Aro	Het	Asph	Carbonates	Carbonates	Carbonates	Sulfates	Sulfides	Sulfates	Nodules
S-2	50	Ca1	r	-26.2	-	-	-	-	-	3.3	1.8	32.7	8.8	-46.3	3.9	11.2
	51	T1	r	-27.0	-	-	-	-	-	3.4	-0.5	30.4	-	-41.4	-	-
	53	T1	r	-27.3	-	-	-	-	-	3.5	-0.8	30.1	10.7	-40.0	6.2	-
	54	T1	r	-	-	-	-	-	-	-	-	-	-	-40.2	-0.4	-
	55	T1	r	-27.0	-	-	-	-	-	2.9	0.1	31.0	-	-39.0	3.7	-
	56	T1	r	-	-	-	-	-	-	-	-	-	-1.4	-39.3	-25.0	-
	57	T1	r	-27.1	-	-	-	-	-	3.3	-0.1	30.8	-0.9	-39.5	-24.4	-
	58	T1	t	-27.0	-	-	-	-	-	-0.9	-1.0	29.9	-	-17.7	7.6	-
	60	T1	t	-27.0	-	-	-	-	-	-0.5	0.1	31.0	11.8	-15.3	6.9	-
	62	T1	o	-26.9	-	-	-	-	-	-0.8	-8.4	22.2	-	-	-	-
PZ-17	5	T1	r	-27.9	-28.2	-28.2	-28.2	-28.0	-28.3	0.9	-4.6	26.3	-	-33.7	-	-
	4	T1	t	-26.6	-27.8	-28.9	-27.8	-27.8	-27.6	-0.4	-4.1	26.8	-	-24.3	-	-
	2	T1	o	-27.3	-28.0	-28.8	-28.0	-27.7	-27.7	-0.2	-4.7	26.2	-	-27.1	-	-
PZ-19	6	T1	r	-27.8	-28.4	-28.6	-28.3	-28.0	-28.5	1.9	-3.6	27.3	-	-36.0	-	7.9
	5	T1	t	-	-	-	-	-	-	-2.1	-3.1	27.8	-	-31.0	-2.8	-
	4	T1	t	-	-	-	-	-	-	-0.4	-4.0	26.9	-	-	-8.5	-
	3	T1	t	-	-	-	-	-	-	0.4	-1.2	29.7	-	-	-	-
	2	T1	o	-	-	-	-	-	-	0.9	0.4	31.3	-	-33.3	5.7	-

Welte, 1984). The significance of those processes is a subject to interpretation; however, the first two suggestions are not tenable because severe water washing and biodegradation was shown to lead to a dramatic depletion of both *n*-alkane and aromatic molecules; the same is true for abiotic oxidation by oxygen (e.g. Charrie-Dehaut *et al.*, 2000). From the data, indicating that oxidised rocks are only partly depleted in hydrocarbons and still contain high amounts of PAH, we tentatively suggest instead that alterations resulted from the action of waters of only slightly oxidative potential. While the oxidised and reduced shales have undergone similar thermal maturation, the high asphaltene and solid bitumen contents in the oxidised rocks suggest that they formed largely as a result of bitumen degradation associated with the passage of oxidising waters and/or deasphalting. Consequently, it is reasonable to conclude that the high concentrations of aromatic hydrocarbons compared to saturated hydrocarbons, the enhanced asphaltenes, the low *n*-alkanes, isoprenoids and resin content, and the high Ph/MPh ratios within the bottommost samples of the Kupferschiefer are caused by influx of oxidising fluids, as described previously for other parts of the Zechstein basin (Püttmann *et al.*, 1989; Bechtel and Püttmann, 1991; Sun and Püttmann, 1997).

ISOTOPIC EVIDENCE FOR AN UPWARD ALTERATION BY OXIDISING FLUIDS

The spread of carbon and oxygen isotope values in the carbonates, which features a gradual enrichment in light isotopes going from the reduced to the oxidised rocks (Fig. 11), implies a strict relationship to the redox of the host rocks and mineralisation type (Fig. 12). Along with the decline in $\delta^{13}C$ and $\delta^{18}O$ values, the copper and silver contents fall, and the gold, platinum and palladium contents rise (*cf.* Figs. 3 and 11). Investigations in the Mansfeld, Sangerhausen, and Richelsdorf deposits indicate that, as in vertical profiles, a lateral increase in the light ^{12}C isotope content (and to a lesser extent the ^{16}O) in the carbonates of the Kupferschiefer, from the pyritiferous zone to the copper-bearing and oxidised rocks, was found. This applies equally to both calcite and dolomite (Bechtel and Püttmann, 1991; Bechtel *et al.*, 2000*a*). The data obtained from the North Sudetic Trough and in other areas of Poland indicate the kerogen of oxidised rocks to be enriched in heavy carbon, which can be explained by the preferential release of hydrocarbons rich in heavy ^{13}C (Püttmann *et al.*, 1993; Bechtel *et al.*, 2000*a*). The revealed dependence of C and O isotope distribution in the organics and carbonates on the metallic facies (Fig. 11) is evidence that, in oxidised and copper-bearing

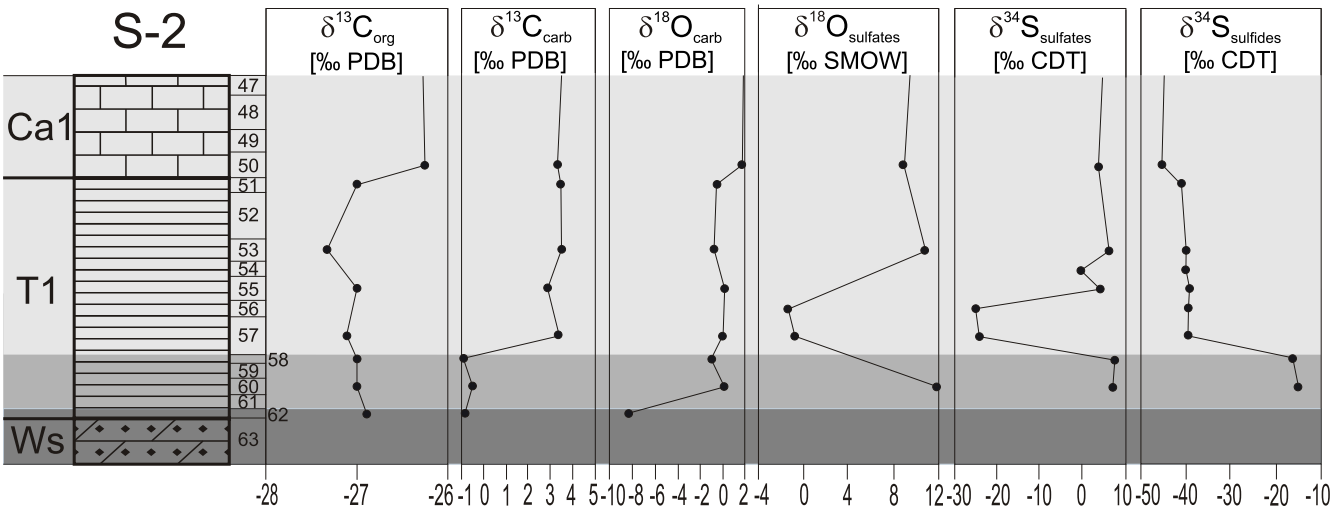

Fig. 11. Variation of σδ13C_{org}, $\delta^{13}C$ and$\delta^{18}O$ in carbonates, $\delta^{34}S$ in sulfides and sulfates, and $\delta^{18}O$ in sulfates from the S-2 section

rocks, this composition was a result of mixing along the flow path of fluids bearing light C and O isotopes through the Kupferschiefer rocks. Since low $\delta^{13}C$ values from carbonates (–2.1 to –0.9‰) are present in oxidised rocks (Table 6) containing C_{org} enriched in the heavy ^{13}C carbon isotope ($\delta^{13}C$ from –27.3 to –26.9‰), it can be thought that light carbon-enriched CO_2 released during the organic matter oxidation was incorporated into the carbonates, giving their ^{12}C enrichment (Fig. 12). A clearer pattern was observed in the Mansfeld, Sangerhausen, Richelsdorf and Lubin-Sieroszowice deposits (Hammer *et al.*, 1990; Bechtel and Püttmann, 1991; Bechtel *et al.*, 2000*a*), where, in the oxidised rocks, the elevated $\delta^{13}C$ values for the organic carbon (–26 to –20‰) fit the lowest $\delta^{13}C$ (–5 to –2‰) and $\delta^{18}O$ (–11 to –5‰) records for the carbonates. Alternatively, ^{13}C- and ^{18}O-depleted hydrothermal water might have come from below (*cf.* Sullivan *et al.*, 1990; Michalik *et al.*, 1998) and interacted with the intervening sediments. The carbon isotope record of the carbonates therefore reflect a mixing of relatively heavy marine Permian carbon ($\delta^{13}C$ from 0 to 2‰) with ^{13}C-depleted organic carbon or supplied from the Rotliegend aquifer.

Until now, the investigation of isotopes of sulfur in the sulfides was performed solely on the reduced rocks. This study provides data for the oxidised shales, thereby permitting a more comprehensive interpretation of the regional alteration. It was shown that the S isotope distribution is characterised by a gradual increase in heavy sulfur (^{34}S) content towards the base of the Kupferschiefer (Fig. 11), which is evidence of enhanced heavy sulfur influx from below. A similar distribution was shown for the Mansfeld deposit (Rösler *et al.*, 1968), where the $\delta^{34}S$ in pyrite and chalcocite vary from –43‰ at the top to –28‰ at the base of the Kupferschiefer profile and also for the Lubin-Sieroszowice deposit (Harańczyk, 1986). A completely different distribution (a gradual increase of ^{34}S from the base to the top of the Kupferschiefer; $\delta^{34}S$ from –45 to –33‰ for pyrite, and from –35 to –29‰ for base-metal sulfides) was found in regions significantly distant from the copper deposits, implying a change from an open system to a closed system (Marowsky, 1969).

Differences in distributions of sulfur isotopes in the oxidised, mineralised and barren (distant from the oxidised area) rocks provokes speculation concerning the source and mechanism of S isotope accumulation, and concerning the reason for such different fractionations of sulfur isotopes having occurred in the different ore types. In the case of the inverse trend revealed in the oxidised areas (Fig. 11), compared to the $\delta^{34}S$ variations for patterns distant from the Rote Fäule, the increase in heavy sulfur content towards the oxidised rocks has to be considered as a result of leaching out of pyrite and early-diagenetic ores from the oxidised rocks and/or their partial replacement by later sulfides, enriched in ^{34}S. Jowett *et al.* (1991*a*, *b*), Oszczepalski (1994), Speczik (1995), Sun and Püttmann (1997) have invoked four main possible sulfur sources leading to the sulfide sulfur isotopic distributions: 1 — bacterial reduction of sulfates (BSR); 2 — pyrite replacement; 3 — organic matter-bound reduced sulfur; 4 — thermochemical sulfate reduction (TSR).

BSR is the common source of reduced sulfur in anoxic sediments (entailing a large negative isotope fractionation up to –60‰), which is considered to be limited to temperatures up to about 60–80°C (Ohmoto, 1986; Machel *et al.*, 1995). The framboidal habit of most of the observed pyrite and its light isotopic composition suggests an origin related to BSR. Systematic variations of $\delta^{34}S$ in pyrite, dependent on distance from the oxidised zones, were not observed (Jowett *et al.*, 1991*a*), which confirms the opinion about its origin being syndiagenetic from BSR. Most pyrite in the anoxic environments is envisaged as forming at shallow burial depths, typically within tens of metres of the sediment-water interface (Curtis, 1980). The scattered $\delta^{34}S$ values of Cu-sulfides, only slightly higher than those of pyrite (Table 6), suggest that a portion of disseminated ores was deposited by BSR, incorporating, like pyrite, ^{32}S-enriched biogenic sulfide. According to Kucha and Pawlikowski (1986), framboid-like Cu sulfides are extremely rare in the

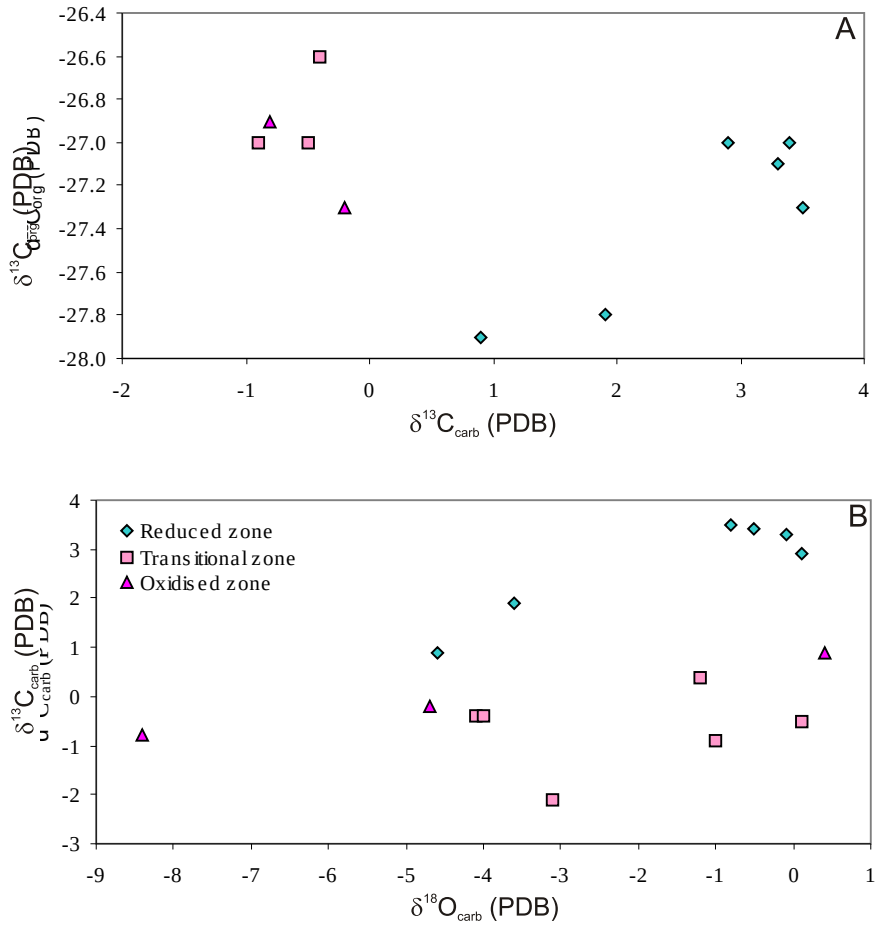

Fig. 12. Carbon and oxygen isotopic composition (PDB) of Kupferschiefer samples from the S-2, PZ-17 and PZ-19 sections

A — plot of $\delta^{13}C_{org}$ vs. $\delta^{13}C_{carb}$; B — plot of $\delta^{13}C_{carb}$ vs. $\delta^{18}O_{carb}$

Lubin-Sieroszowice deposit. Mayer and Piestrzyński (1985) suggested that such spheres preferentially resulted from the replacement of carbonate spheroids, whereas Sawłowicz (1990) considered the copper sulfide framboids as syndiagenetic precipitates. As shown by numerous Cu-sulfide framboids at the reduced side of the redox front, early diagenetic framboidal pyrite could have been replaced by Cu-sulfides (Oszczepalski, 1989, 1999; Sun *et al.*, 1995). The absence of pyrite framboids at the base of reduced interval, accompanied by the presence of light S-enriched ore pseudomorphs after pyrite (Fig. 4), suggests that the conversion of precursor pyrite to Cu-sulfides was apparently the essential mode of copper deposition. Studies of sulfur isotopes showing a rise in heavy sulfur content in the sulfides of the oxidised rocks and within the base of the reduced interval suggest a supply of isotopically heavier sulfur due to thermal (at temperatures > 50°C) decomposition of S-containing organic matter (Rospondek *et al.*, 1994) or from the abiogenic reduction of ore fluid sulfates (Jowett *et al.*, 1991*b*), that appears to be common in geologic settings with temperatures of about 80–140°C (Machel *et al.*, 1995). Thermal decomposition of organically bound sulfur usually provides negligible amounts of sulfur, whereas TSR may contribute high concentrations of H_2S (Ohmoto, 1986) and was considered as a mechanism promoting formation of the Kupferschiefer deposits (Bechtel and Püttmann 1991; Jowett *et al.*, 1991*b*). While arguments persist over the relevance of TSR to the late-diagenetic Kupferschiefer system, the strongly negative $\delta^{34}S$ values of Cu-sulfides are not entirely consistent with the TSR model, unless we assume that most of the sulfates hypothetically reduced by organic matter would have come from oxidation of the ^{32}S-enriched sulfides. Low temperature oxidation of sulfides and slightly higher temperature hydration of pyrite may result in the formation of aqueous sulfate which has a $\delta^{34}S$ value essentially the same as that of pyrite (Ohmoto, 1986; Machel *et al.*, 1995). However, TSR was ineffective as long as reduced S could have been supplied from pyrite (Sun and Püttmann, 1997). Therefore, it is thought that TSR was not the most significant metal-fixing reaction but rather an accompanying alteration process induced by flow of oxidising solutions, following the main copper emplacement.

Our results obtained during this study and the data sets gathered previously (Wodzicki and Piestrzyński, 1994) show that it is possible to distinguish four sulfide groups identified by their average $\delta^{34}S$ values: pyrite (–35‰), disseminated ores

(–34‰), coarse-grained and vein ores (–30‰), and massive ores (–18‰). Marowsky (1969) also reported that the copper sulfides contain more heavy sulfur ($\delta^{34}S$ from –38 to –23‰) than pyrite ($\delta^{34}S$ from –41 to –28‰). Significant enrichment of the coarse-grained and veinlet copper sulfides (in the range –36.3 to –16.8‰) than in the disseminations suggests that the disseminated ores contain more biogenic sulfur (Sawłowicz, 1989*b*; Jowett *et al.*, 1991*a*; Harańczyk, 1986). In general, it is not possible to discern fundamental differences between the pre-compactional and post-compactional pyrite, although locally (*cf.* Jowett *et al.*, 1991*b*) heavy sulfur enrichment was registered for the pyrite nodules ($\delta^{34}S$ –25.2‰) relative to the framboidal pyrite ($\delta^{34}S$ –40.6‰). Thus, the gradually increasing heavy sulfur content, successively in the disseminated, coarse-grained, vein and massive sulfides, might be explained by abiogenic reduction of sulfates derived from both oxidised isotopically-light sulfides and from isotopically-heavy sulfur from sulfate-containing ore fluids, resulting in the preferential accumulation of heavy sulfur in the late-diagenetic sulfides.

The mixed sulfur sources are clearly indicated by the isotopic spread of trace, finely disseminated sulfates; the $\delta^{34}S$ values range from slightly negative to slightly positive indicating that these sulfates contain both sulfur typical for the Permian sedimentary sulfates as well as light sulfur from pyrite oxidation. It seems that the fractionation of the sulfur and oxygen isotopes in the trace sulfates is suggestive of advanced reactions between the oxidising mineralising fluids and pyrite. The most ^{34}S-depleted sulfates in the reduced samples directly overlying the oxidised rocks and at the top of TZ (Table 6; Fig. 11) argue for migration of the oxidising fluids towards the top of the profile. The formation of a significant proportion of sulfate in this interval produced by oxidation of sulfides is unequivocally supported also by the low $\delta^{18}O$ values from sulfate, apparently different from the Zechstein marine range, which is 8–13‰ SMOW. The ore fluids were characterised by δD values ranging from –23 to –3‰ (SMOW) and $\delta^{18}O$ between 2 and 7‰ (SMOW) (Bechtel *et al.*, 2000*b*), which argue that these brines, initially meteoric or marine waters, became saline and isotopically evolved either by evaporation, dissolution of salt or mixing with connate fluids (Bechtel *et al.*, 2000*b*). This characteristic is in accordance with previous suggestions (Kucha and Pawlikowski, 1986; Tonn *et al.*, 1987; Sawłowicz, 1989*b*; Wodzicki and Piestrzyński, 1994; Michalik *et al.*, 1998). The $\delta^{34}S$ record in anhydrite nodules (7 to 12‰, Table 6) is similar to the values in the anhydrites of the first Zechstein cyclothem ($\delta^{34}S$ from 11.3 to 12.1‰) and in the sulfates present in the Rotliegend redbeds ($\delta^{34}S$ from 5.9 to 9.8‰; Jowett *et al.*, 1991*a*, *b*; Peryt and Scholle, 1996; Michalik *et al.*, 1998), indicating that nodular sulfates were recycled from Permian sedimentary anhydrite.

ROLE OF OXIDATION IN THE FORMATION OF ORES

The variation in composition, alteration of organic matter and isotopic differences reflect possible interactions with mineralising solutions and seems to be a function of the intensity of hydrothermal circulation. The results of these changes are the redox-related variations in C_{org}, maceral composition, hydrocarbons and non-hydrocarbon compounds, and in the isotopic composition of the kerogen, bitumen, hydrocarbons, sulfates and sulfides (Figs. 3, 5, 6 and 11). The pervasive degradation of organic material and sulfides in oxidised rocks and the less advanced degradation in the TZ (Figs. 4 and 5) clearly confirm that the alteration caused by the mineralising fluids weakened in an upward direction.

It is generally accepted that the ores were mobilised by oxidising (in the hematite stability field) Na-Ca-Cl basinal brines, originating within the underlying Rotliegend redbeds by convection (Jowett, 1986; Oszczepalski, 1989), salt doming (Kucha and Pawlikowski, 1986) or direct expulsion (Cathles *et al.*, 1993). Consequently, both convective thermal- and compaction-driven upwelling flows of metalliferous fluids have been invoked as possible mechanisms for the formation of Kupferschiefer-type deposits. While the Wolsztyn Ridge (Karnkowski, 1999) acted as a barrier for a long-distance lateral fluid flow, the role of halocinetically geopressured brine migration in the formation of the Lubin-Sieroszowice deposit (Kucha and Pawlikowski, 1996) must have been largely limited. Wodzicki and Piestrzyński (1994), as well as Piestrzyński and Wodzicki (2000) have expanded on the Kucha and Pawlikowski (1986) idea that precipitation of metals took place along the interface between the ascending oxidising fluids and a reducing fluid descending from the overlying evaporites. However, this proposition offered no geochemical and isotope data supporting the role of descending fluids, and, indeed, downward fluid infiltration is unlikely during basin compaction (e.g. de Caritat, 1989), which must have resulted from the Late Permian-Jurassic syn-rift and post-rift subsidence of the extensional Polish Trough (Karnkowski, 1999; van Wees *et al.*, 2000).

The association of Cu-Ag orebodies with the redox edge of the post-depositional Rote Fäule unit may be explained by superposition of the early diagenetic low-grade mineralisation and high-grade accumulations formed by ascending ore fluids and redistribution of earlier-formed sulfides. Under this scenario, the most intensive flow of mineralising fluids took place in the western parts of the Lubin-Sieroszowice deposit, where locally the entire Kupferschiefer series was converted to Rote Fäule. The irregular nature of the oxidation front appear to imply different intensities of upward and lateral fluid incursions and the oxidative alteration both on a mine and regional scale (Fig. 1). The mineralising fluids reacted with the rocks, resulting in evolution of the Eh-pH conditions of the solutions as they migrated through the basal Zechstein. Spatial and textural relationships suggest that both base and noble metals were transported in slightly oxidising and acidic, chloride brines and precipitated during ore-forming process involving metal redistribution. It is well documented that organic- and reduced sulfur-rich host rocks are highly efficient traps for base metals. As suggested earlier, in most natural systems dominated by oxidised species such as hematite, gold and PGE are preferentially transported as chloride complexes, which can be destablilised by reaction with reducing agents, causing precipitation of precious metals. It is therefore reasonable to assume that organics, pyrite and copper sulfides promoted deposition of gold and PGM in primarily reduced Kupferschiefer sediments, but exclusively in areas where the basal Zechstein sediments were thought to have been extensively flushed by upwelling basinal

waters. The same fluids may have aided subsequently an adsorption of precious metals by iron oxides. Upon oxidation, Au, Pt and Pd were remobilised and reprecipitated, whereas Cu and Ag were removed away from the Rote Fäule. The result is that the mineralised interval cuts across the strata parallel to the redox front and underlies the Cu-Ag horizon (Fig. 3), the Au-Pt-Pd mineralisation forms a belt rimming the reduced areas, and the Kupferschiefer sediments distant from the feeder areas are not mineralised with precious metals (Fig. 1).

In a system dominated by the Rotliegend formation brines, certain amounts of oxygen needed for the destruction of pyrite, Cu sulfides and organic matter could have come from meteoric water, descending in the Zechstein in association with subaerial exposure (Jowett *et al.*, 1991*b;* Peryt and Scholle, 1996; Oszczepalski and Rydzewski, 1997). Pyrite oxidation by ferric iron would be expected to dominate in oxygen-poor waters. Other potential oxidants might have been oxyanions of sulfur, Fe^{2+}, Cu^{2+}, Cu^{+}, Au^{3+} and radicals produced during radiolysis of aqueous fluids (Kucha, 1990; Oszczepalski, 1994; Kucha and Przybyłowicz, 1999). Under higher temperatures, estimated around 100°C, oxidation of organics would accompany sulfate reduction, involving CO_2, H_2S and hydrocarbons (Ohmoto, 1986; Machel *et al.*, 1995). Despite the abundant biogenic sulfur in the Kupferschiefer, the $\delta^{34}S$ spreads for copper sulfides (Fig. 11) imply that some additional heavy sulfur could have been provided by sulfates leached from the underlying Rotliegendes, by extrinsic H_2S-containing hydrocarbons or from the oxidation of organic sulfur (Jowett *et al.*, 1991*b*). This is not in accordance with the opinion that copper mineralisation is syndiagenetic and occurred by BSR in an open system changing gradually into a closed system (*cf.* Sawłowicz, 1989*c*, 1990), although the earliest stage of diagenesis involving BSR was possibly coeval with the precipitation of small amounts of base-metal sulfides. As mentioned above, certain amounts of reduced sulfur could have been added to the system during late diagenesis, as a result of TSR (Püttmann *et al.*, 1989; Bechtel and Püttmann, 1991; Jowett *et al.*, 1991*b*; Speczik, 1995; Sun and Püttmann, 1997; Sun, 1998). As abiogenic sulfate reduction may cause changes in the chemical composition of organic matter and host minerals (oxidation of hydrocarbons, hydrogen depletion, bitumen deposition, deasphalting, calcitisation) and provides heavy (^{34}S) sulfur (Machel *et al.*, 1995), the compositions characterising the Rote Fäule may be postulated to have been partly caused by TSR. The occurrence of patchy type Cu sulfides intimately associated with solid bitumen and sparry calcite in the mineralised rocks (Sun, 1998) is suggestive of the TSR participation in sulfide precipitation. Bitumens being by-products of the main mineralisation event could have become a source of hydrogen during TSR (Püttmann *et al.*, 1989; Bechtel and Püttmann, 1991; Bechtel *et al.*, 2000*a*).

The organic material in the studied rocks has a moderate level of thermal maturity. The reflectance of non-recycled vitrinite (collinite) varies from 0.72 to 1.13% (Table 2), with the R_o increase in the oxidised rocks. As suggested earlier (Speczik and Püttmann, 1987; Oszczepalski, 1989; Wolf *et al.*, 1989; Sun *et al.*, 1995; Sun and Püttmann, 1997; Koch, 1997), elevated R_o values are assumed to be related to changes caused by oxidation processes. The relatively low reflectance of non-recycled macerals (Table 2) indicates a maximum palaeotemperature of 90–120°C, which means that the temperature of the mineralising fluids did not exceed these values, but still was within the range allowing the formation of low temperature chalcocite and inorganic reduction of sulfates. Geological evidence imply that the threshold for TSR lies between 80–140°C, although rock, theoretical and experimental studies suggest that in some settings temperatures of 160–180°C appear to be necessary (e.g. Machel *et al.*, 1995). Corresponding maximum palaeotemperatures ranging from 60 to 150°C are suggested in different parts of the Zechstein basin by the *n*-alkane composition (90–140°C, Gondek, 1980), the fluid inclusions in the calcite cement of Weissliegendes sandstones (120°C, Tonn *et al.*, 1987), the S isotope composition in the bornite-chalcopyrite veinlets (60–90°C, Jowett *et al.*, 1991*b*) and the isotope study of the hydroxyl illite group (100–150°C, Bechtel *et al.*, 2000*b*). The maximum burial temperature of the Zechstein base in the Lubin area, based on a normal heat flow, was in the range 60–80°C (Jowett, 1986; Karnkowski, 1999) indicating that the maximum occurred as the effect of ascendant fluids during the thermal event corresponding likely with Triassic rifting (Jowett, 1986).

That the Kupferschiefer ores are of early-to-late diagenetic origin is evidenced by the hematite dating (250–220 Ma; Jowett *et al.*, 1987), modified to 255–245 Ma (Nawrocki, 2000), and authigenic illite dating (216–190 Ma; Bechtel *et al.*, 1999, 2000*b*). Kucha and Przybyłowicz (1999) suggested an 180–175 Ma age of thucholite nodules and considered the upper limit for the time of mineralisation, set by the age of amalgams, as Early Cretaceous. Hence, the formation of the Zechstein Rote Fäule/ore system can be constrained to the time period between 258 Ma (the depositional age of the Kupferschiefer) and the Early Cretaceous. The formation of the observed Lubin-Sieroszowice deposit, however, is rather thought to have pertained during the post-Zechstein Triassic rifting by brine recirculation or superposition of early- and late-diagenetic mineralisation (Cathles *et al.*, 1993).

CONCLUSIONS

Petrographic, geochemical and isotopic studies on Kupferschiefer samples at the contact of the oxidised and reduced lithologies in the western part of the Lubin-Sieroszowice mining district confirm an extensive oxidation of initially reduced shales. The alteration of the reduced rocks is particularly intense in the basal part of the Kupferschiefer horizon, from which the major portion of the organic matter indigenous to the host rocks was removed. Thus, there are lines of evidence that the Rote Fäule resulted from the upward advancing post-depositional oxidation of organic-rich basal Zechstein. The altering fluids caused depletion of kerogen in hydrogen equivalents, the aromatisation of bitumen and the removal of saturated hydrocarbons from the liptinites and their lipid-rich precursors, leaving behind a spent carbonaceous residue. As a result, a distinct downward decline in the C_{org}, bitumens and unstable macerals contents is observed. HI and Ph/MPh indices and vitrinite reflectance values readily parallel this trend.

Due to oxidation, organic matter in the oxidised shales was transformed into degraded aromatic-rich type III kerogen. Bitumen (EOM) occurs in negligible amounts in these rocks and is characterised by low hydrocarbon, *n*-alkane, isoprenoid and resin contents and also by high concentrations of heavy aromatic hydrocarbons and asphaltenes. The organic constituents are dominated by solid bitumen, whereas alginites are absent and collinites, bituminites and liptodetrinites are minor constituents. Non-recycled vitrinite in the oxidised rocks shows the highest reflectance. Distinct stable isotope characteristics indicate a clear tendency of ^{13}C-enrichment in the oxidised kerogen, accompanied by a depletion of ^{13}C and ^{18}O in the carbonates. The spread of Cu-sulfides S-isotopic values is interpreted as a mixing of two main reduced sulfur sources: isotopically light biogenic sulfur and heavier sulfur from incoming fluids. Heavy sulfur isotope enrichment in the sulfides within the oxidised zone may reflect abiogenic reduction of ore fluid sulfate. ^{34}S- and ^{18}O-depleted sulfates are present at the boundary between the transitional and reduced zone implying a significant oxidation of sulfides. Most of the base metals (Cu, Ag, Pb, Zn, Co, Mo, Ni, Ta and As) were removed from the oxidised lithologies, whereas Au, Pt, Pd, V, Se, REE (partly U and Hg) concentrated within the Rote Fäule units. The intimate spatial association of the precious metals with the hematisation suggests that oxidative alteration played a crucial role in Au, Pt and Pd location at the oxidation front. The ultimate location of the oxidation front is represented by the position of the transition zone, which is typically characterised by the highest concentrations of PAHs, enhanced dibenzothiophene contents and the highest Ph/MPh and V/Cr ratios.

This study confirms that the boundary between the reduced and oxidised rocks separates sulfidic Cu-Ag ores from the Rote Fäule-related Au-Pt-Pd mineralisation. At the oxidation front, Cu-Ag mineralisation prevails, dominated by Cu-S type sulfides (chalcocite, digenite, and covellite), and followed upwards by Cu-Fe-S mineralisation. Possible explanation for this succession include significant interaction of upward migrating mineralising fluids with organic matter and sulfides-rich rocks undergoing alteration and the weakening redox potential of advancing fluids as they evolved through time. As a result, on the oxidised side of the redox front, there are only relics of the copper sulfides, accompanied by iron oxides (mainly hematite pseudomorphs after pyrite framboids) and the Au-Pt-Pd mineralisation coincides herein with hematite mineralisation and organic carbon loss. The correspondence of the precious metal mineralisation with the occurrence of solid bitumens suggests that the bitumens could have acted as an additional reductant, preferentially scavenging precious metals from incoming solutions.

The observed alteration geochemistry and petrology provide evidence for an ascending post-depositional flow of low-temperature (< 150°C) hydrothermal oxidising metal-bearing fluids. The progressive expansion of oxidation is clearly manifested by its cutting-across the strata and the gradual variation of the chemical, mineralogical and maceral composition within the transition zone. As the mineralising processes continued, the Rote Fäule-ore interface migrated higher in the basal Zechstein sequence and farther out into the basin, accounting for metal zoning and increasing the size and grade of the Au-Pt-Pd and Cu-Ag deposits until fluid circulation ceased.

Acknowledgements. We are indebted to M. Kotarba (University of Mining and Metallurgy, Cracow) and H. Strauss (Lehrstuhl für Sediment- und Isotopengeologie, Ruhr-Universität, Bochum) for supervising Rock-Eval pyrolysis and isotope analyses of the PZ-17 and PZ-19 samples, respectively. Supervision of analytical procedures by A. Bellok, Z. Dobieszyńska, K. Hnatyszak, I. Iwasińska-Budzyk, D. Karmasz, P. Pasławski, A. Sztuczyńska (PGI) and H. Otwinowska (ICHP) is greatly appreciated. K. Niczyporuk and A. Saternus provided valuable advice concerning software. Discussions with A. C. Brown, R. Gratzer, A. Rydzewski and S. Speczik were particularly helpful. W. Püttmann and W. C. Elliott are gratefully acknowledged for their constructive reviews. Support to SO was provided by the National Committee for Scientific Research, Grant No. 9 T12B 014 19.

REFERENCES

BECHTEL A., ELLIOTT W. C., WAMPLER J. M. and OSZCZEPALSKI S. (1999) — Clay mineralogy, crystallinity, and K-Ar ages of illites within the Polish Zechstein Basin: implications for the age of Kupferschiefer mineralization. Econ. Geol., **94**: 261–272.

BECHTEL A., GHAZI A. M., ELLIOTT W. C. and OSZCZEPALSKI S. (2001*a*) — The occurrences of the rare earth elements and the platinum group elements in relation to base metal zoning in the vicinity of Rote Fäule in the Kupferschiefer of Poland. Appl. Geochem., **16**: 375–386.

BECHTEL A., GRATZER R., PÜTTMANN W. and OSZCZEPALSKI S. (2000*a*) — Gechemical and isotopic composition of organic matter in the Kupferschiefer of the Polish Zechstein basin: relation to maturity and base metal mineralization. Int. J. Earth Sc., **89**: 72–89.

BECHTEL A., GRATZER R., PÜTTMANN W. and OSZCZEPALSKI S. (2001*b*) — Variable alteration of organic matter in relation to metal zoning at the Rote Fäule front (Lubin-Sieroszowice mining district, SW Poland). Org. Geochem., **32**: 377–395.

BECHTEL A. and PÜTTMANN W. (1991) — The origin of the Kupferschiefer-type mineralization in the Richelsdorf Hills, Germany, as deduced from stable isotope and organic geochemical studies. Chem. Geol., **91**: 1–18.

BECHTEL A., SHIEH Y.-N., ELLIOTT W. C., OSZCZEPALSKI S. and HOERNES S. (2000*b*) — Mineralogy, crystallinity and stable isotopic composition of illitic clays within the Polish Zechstein basin: implications for the genesis of Kupferschiefer mineralization. Chem. Geol., **163**: 189–205.

CATHLES L. M. III., OSZCZEPALSKI S. and JOWETT E. C. (1993) — Mass balance evaluation of the late diagenetic hypothesis for Kupferschiefer Cu mineralization in the Lubin basin of southwestern Poland. Econ. Geol., **88**: 948–956.

CHARRIE-DEHAUT A., LEMOINE S., ADAM P., CONNAN J. and ALBRECHT P. (2000) — Abiotic oxidation of petroleum bitumens under natural conditions. Org. Geochem., **31**: 977–1003.

CURIALE J. A. (1986) — Origin of solid bitumens, with emphasis on biological marker results. Org. Geochem., **10**: 559–580.

CURTIS C. D. (1980) — Diagenetic alteration in black shales. J. Geol. Soc. London, **137**: 189–194.

De CARITAT P. (1989) — Note on the maximum upward migration of pore water in response to sediment compaction. Sediment. Geol., **65**: 371–377.

ESPITALIE J., DEROO G. and MARQUIS F. (1985) — La pyrolyse Rock Eval et ses applications. Rev. Inst. Franc. Petrole, **40–41**: 563–579.

EZRA S., FEINSTEIN S., PELLY I., BAUMAN D. and MILOSLAVSKY I. (2000) — Weathering of fuel oil spill on the east Mediterranean coast, Ashdod, Israel. Org. Geochem., **31**: 1733–1741.

GALIMOV E. M. (1980) — 13C/12C ratios in kerogen. In: Kerogen — Insoluble Organic Matter from Sedimentary Rocks (ed. B. Durand): 271–299.

GAMMONS C. H. (1995) — Experimental investigations of the hydrothermal geochemistry of platinum and palladium: IV. The steichiometry of Pt(IV) and Pd(II) chloride complexes at 100 to 300°C. Geochim. Cosmochim. Acta, **59**: 1655–1667.

GOLDHABER M. B. (1983) — Experimental study of metastable sulphur oxyanion formation during pyrite oxidation at pH 6–9 and 30°C. Am. J. Sc., **283**: 193–217.

GONDEK B. (1980) — Geochemistry of *n*-alkanes occuring in the sediments of the Polish Lowlands. Prace Inst. Geol., **97**: 1–42.

HALL G. E. M., PELCHAT J.-C. and LOOP J. (1988) — Separation and recovery of various sulphur species in sedimentary rocks for stable sulphur isotopic determination. Chem. Geol., **67**: 35–45.

HAMMER J., JUNGE F., RÖSLER S., NIESE S., GLEISBERG B. and STIEL G. (1990) — Element and isotope geochemical investigations of the Kupferschiefer in the vicinity of "Rote Fäule", indicating copper mineralization (Sangerhausen basin, G.D.R.). Chem. Geol., **85**: 345–360.

HARAŃCZYK C. (1986) — Zechstein copper-bearing shales in Poland. Lagoonal environments and sapropel model of genesis. In: Geology and Metallogeny of Copper Deposits (eds. G. Friedrich *et al*.). **46**: 462–476.

HYLAND M. M. and BANCROFT G. M. (1990) — Palladium sorption and reduction on sulphide mineral surfaces: an XPS and AES study. Geochim. Cosmochim. Acta, **54**: 117–130.

INTERNATIONAL COMMITTEE FOR COAL AND ORGANIC PETROLOGY (1993) — International Handbook of Coal Petrography. 2nd ed., 3rd suppl. Univ. Newcastle Upon Tyne, England.

JACOB H. (1989) — Classification, structure, genesis and practical importance of natural solid bitumen ("migrabitumen"). Int. J. Coal Geol., **11**: 61–79.

JAIRETH S. (1992) — The calculated solubility of platinium and gold in oxygen-saturated fluids and the genesis of platinium-palladium and gold mineralization in the unconformity-related uranium deposits. Mineral. Deposita, **27**: 42–54.

JOWETT E. C. (1986) — Genesis of Kupferschiefer Cu-Ag deposits by convective flow of Rotliegende brines during Triassic rifting. Econ. Geol., **81**: 1823–1837.

JOWETT E. C., PEARCE G. W. and RYDZEWSKI A. (1987) — A Mid-Triassic paleomagnetic age of the Kupferschiefer mineralization in Poland based on a revised apparent polar wander path of Europe and Russia. J. Geoph. Res., **92**: 581–598.

JOWETT E. C, ROTH T., RYDZEWSKI A. and OSZCZEPALSKI S. (1991*a*) — "Background" delta 34S values of Kupferschiefer sulfides in Poland: pyrite-marcasite nodules. Mineral. Deposita, **26**: 89–98.

JOWETT E. C., RYE R. O., OSZCZEPALSKI S. and RYDZEWSKI A. (1991*b*) — Isotopic evidence for the addition of sulfur during formation of the Kupferschiefer ore deposits in Poland. Zbl. Geol. Palaont., I, **4**: 1001–1015.

KARNKOWSKI P. H. (1999) — Origin and evolution of the Polish Rotliegend basin. Polish Geol. Inst. Spec. Papers, **3**: 1–93.

KOCH J. (1997) — Organic petrographic investigations of the Kupferschiefer in northern Germany. Int. J. Coal Geol., **33**: 301–316.

KUCHA H. (1981) — Precious metal bearing shale from Zechstein copper deposits, Lower Silesia, Poland. Trans. Instn. Min. Metal., **92**: B72–B79.

KUCHA H. (1990) — Geochemistry of the Kupferschiefer, Poland. Geol. Rundsch., **79**: 387–399.

KUCHA H. (1995) — Redefinition of Rote Fäule, Kupferschiefer, Poland. In: Mineral Deposits (eds. J. Pasava, B. Kribek and K. Zák): 953–956.

KUCHA H. and PAWLIKOWSKI M. (1986) — Two-brine model of the genesis of strata-bound Zechstein deposits (Kupferschiefer type), Poland. Mineral. Deposita, **25**: 262–271.

KUCHA H. and PRZYBYŁOWICZ W. (1999) — Noble metals in organic matter and clay-organic matrices, Kupferschiefer, Poland. Econ. Geol., **94**: 1137–1162.

LANDIS C. R. and CASTANO J. R. (1994) — Maturation and bulk chemical properties of a suite of solid hydrocarbons. Org. Geochem., **22**: 137–149.

MACHEL H. G., KROUSE H. R. and SASSEN R. (1995) — Products and distinguishing criteria of bacterial and thermochemical sulfate reduction. Appl. Geochem., **10**: 373–389.

MACHESKY M. L., ANDRADE W. O. and ROSE A. W. (1991) — Adsorption of gold(III)-chloride and gold(I)-thiosulfate anions by goethite. Geochim. Cosmochim. Acta, **55**: 769–776.

MAROWSKY G. (1969) — Schwefel-, Kohlenstoff- und Sauerstoff-Isotopenuntersuchungen am Kupferschiefer als Beitrag zur genetischen Deutung. Contr. Mineral. Petrol., **22**: 290–334.

MAYER W. and PIESTRZYŃSKI A. (1985) — Ore minerals from Lower Zechstein sediments at Rudna mine, Fore-Sudetic Monocline, SW Poland. Prace Mineral., **75**: 1–72.

MICHALIK M. (1979) — Spotted rocks (Rote Fäule) in the Zechstein Z-1 south of Głogów (Poland). Prace Mineral., **54**: 23–35.

MICHALIK M., JĘDRYSEK M. O., WEBER-WELLER A., KAŁUŻNY A. and HAŁAS S. (1998) — Origin of some diagenetic solutions in the Weissliegendes sandstone in SW Poland: preliminary stable isotope studies of carbonate and sulfate cements. RMZ, **45**: 118–123.

MYCROFT J. R., BANCROFT G. M., Mc INTYRE N. S. and LORIMER J. W. (1995) — Spontaneous deposition of gold on pyrite from solutions containing Au(III) and Au(I) chlorides. Part I: a surface study. Geochim. Cosmochim. Acta, **59**: 3351–3365.

NAWROCKI J. (2000) — Clay mineralogy, crystallinity, and K-Ar ages of illites within the Polish Zechstein Basin: implications for the age of Kupferschiefer mineralization — a discussion. Econ. Geol., **95**: 241–242.

NEWTON R. J., BOTTRELL S. H., DEAN S. P., HATFIELD D. and RAISWELL R. (1995) — An evaluation of use of the chromous chloride reduction method for isotopic analyses of pyrite in rocks and sediment. Chem. Geol., **125**: 317–320.

OHMOTO H. (1986) — Stable isotope geochemistry of ore deposits. Rev. Miner., **16**: 491–559.

OSZCZEPALSKI S. (1989) — Kupferschiefer in southwestern Poland: sedimentary environments, metal zoning, and ore controls. GAC Spec. Paper, **36**: 571–600.

OSZCZEPALSKI S. (1994) — Oxidative alteration of the Kupferschiefer in Poland: oxide-sulfide parageneses and implications for ore-forming models. Geol. Quart., **38** (4): 651–672.

OSZCZEPALSKI S. (1999) — Origin of the Kupferschiefer polymetallic mineralization in Poland. Mineral. Deposita, **34**: 599–613.

OSZCZEPALSKI S. and RYDZEWSKI A. (1991) — The Kupferschiefer mineralization in Poland. Zbl. Geol. Paläont., I, **4**: 975–999.

OSZCZEPALSKI S. and RYDZEWSKI A. (1997) — Metallogenic atlas of the Zechstein copper-bearing series in Poland. Państw. Inst. Geol., Warszawa.

OSZCZEPALSKI S. and RYDZEWSKI A. (1998) — Gold, platinum and palladium in the Lubin-Sieroszowice deposit based on boreholes. PTMin. Prace Spec., **10**: 51–70.

OSZCZEPALSKI S., PIESTRZYŃSKI A., RYDZEWSKI A., SPECZIK S. and NICZYPORUK K. (1997) — Exploration of the Au-Pt-Pd Zechstein mineralization in SW Poland. In: Noble Metals in NE Part of the Bohemian Massif and its Surroundings — Genesis, Distribution, and Perspectives (ed. A. Muszer): 48–55. Konf. Naukowa Jarnołtówek 19–21 czerwiec 1997, Wrocław.

PERYT T. M. and SCHOLLE P. A. (1996) — Regional setting and role of meteoric water in dolomite formation and diagenesis in an evaporite

basin: studies in the Zechstein (Permian) deposits of Poland. Sedimentology, **43**: 1005–1024.

PIESTRZYŃSKI A. and PIECZONKA J. (1997) — Gold and PGE on an oxide-reducing interface in Lower Zechstein sediments of the Fore-Sudetic Monocline, SW Poland. In: Mineral Deposits (ed. H. Papunen): 99–102.

PIESTRZYŃSKI A., PIECZONKA J., SPECZIK S., OSZCZEPALSKI S. and BANASZAK A. (1997) — Noble metals from the Kupferschiefer-type deposits, Lubin-Sieroszowice, SW Poland. In: Mineral Deposits (ed. H. Papunen): 563–566.

PIESTRZYŃSKI A. and WODZICKI A. (2000) — Origin of the gold deposit in the Polkowice-West mine, Lubin-Sieroszowice Mining District, Poland. Mineral. Deposita, **35**: 37–47.

PÜTTMANN W., BECHTEL A., SPECZIK S. and FERMONT W. J. J. (1993) — Combined application of various geochemical methods on Kupferschiefer of the North-Sudetic Syncline, SW Poland: evidence for post-depositional accumulation of copper and silver. In: Current Research in Geology Applied to Ore Deposits (eds. Fenoll Hach-Ali, Torres-Ruiz and Gervilla): 213–216.

PÜTTMANN W., FERMONT W. J. J. and SPECZIK S. (1991) — The possible role of organic matter in transport and accumulation of metals exemplified at the Permian Kupferschiefer formation. Ore Geol. Rev., **6**: 563–579.

PÜTTMANN W., MERZ C. and SPECZIK S. (1989) — The secondary oxidation of organic material and its influence on Kupferschiefer mineralization of southwest Poland. Appl. Geochem., **4**: 151–161

RENTZSCH J. (1974) — The Kupferschiefer in comparison with the deposits of the Zambian Copperbelt. In: Gisements Stratiformes et Provinces Cupriferes (ed. P. Bartholome). Soc. Geol. Belg: 395–418.

ROBERT P. (1981) — Classification of Organic Matter by means of fluorescence; application to hydrocarbon source rocks. Int. J. Coal Geol., **1**: 101–137.

ROMBERGER S. B. (1988) — Geochemistry of gold in hydrothermal deposits. U. S. Geol. Survey Bull., **1857-A**: 9–25.

ROSENBAUM J. and SHEPPARD S. M. F. (1986) — An isotopic study of siderites, dolomites and ankerites at high temperatures. Geochim. Cosmochim. Acta, **50**: 1147–1150.

ROSPONDEK M. J., FIJAŁKOWSKA A. and LEWANDOWSKA A. (1993) — The origin of organic matter in Lower Silesian copper-bearing shales. Ann. Soc. Geol. Pol., **63**: 85–99.

ROSPONDEK M. J., De LEEUW J. W., BAAS M., Van BERGEN P. F. and LEEREVELD H. (1994) — The role of organically bound sulfur in stratiform ore sulfide deposits. Org. Geochem., **21**: 1181–1191.

RÖSLER H. J., PILOT J., HARZER D. and KRÜGER P. (1968) — Isotopengeochemische Untersuchungen (O, S, C) an Salinar- und Sapropelsedimenten Mitteleuropas. 23rd IGC Proc., **6**: 89–100.

RYDZEWSKI A. (1969) — Petrography of the copper-bearing Zechstein shales in the Fore-Sudetic Monocline (Lower Silesia). Biul. Inst. Geol., **217**: 113–167.

RYDZEWSKI A. (1978) — Oxidated facies of the copper-bearing Zechstein shales in the Fore-Sudetic Monocline. Prz. Geol., **26** (2): 102–108.

SAKAI H. and KROUSE H. R. (1971) — Elimination of memory effect in ^{16}O–^{18}O determination in sulfates. Earth. Planet. Sc. Lett., **11**: 369–373.

SAWŁOWICZ Z. (1989*a*) — Organic matter in the Zechstein Kupferschiefer from the Fore-Sudetic Monocline. I. Bitumen. Mineral. Polon., **20**: 69–86.

SAWŁOWICZ Z. (1989*b*) — Isotopic composition of C, O, S in the organic-rich copper-bearing shale from the Kupferschiefer in Poland. Arch. Mineral., **54**: 5–19.

SAWŁOWICZ Z. (1989*c*) — On the origin of copper mineralization in the Kupferschiefer: a sulfur isotope study. Terra Nova, **1**: 339–343.

SAWŁOWICZ Z. (1990) — Primary copper sulphides from the Kupferschiefer, Poland. Mineral. Deposita, **25**: 262-271.

SAWŁOWICZ Z. (1991) — Organic matter in the Zechstein Kupferschiefer from the Fore-Sudetic Monocline. II. Kerogen. Mineral. Polon., 22: 49-67.

SOFER Z. (1984) — Stable carbon isotope compositions of crude oils: application to source depositional environments and petroleum alteration: AAPG Bull., **68**, 31–49.

SPECZIK S. (1994) — Kupferschiefer mineralization in the light of organic geochemistry and coal petrology studies. Geol. Quart., **38** (4): 639–650.

SPECZIK S. (1995) — The Kupferschiefer mineralization of Central Europe: new aspects and major areas of future research. Ore Geol. Rev., **9**: 411–426.

SPECZIK S. and PÜTTMANN W. (1987) — Origin of Kupferschiefer mineralization as suggested by coal petrology and organic geochemical studies. Acta Geol. Pol., **37**: 167–187.

SPECZIK S., RYDZEWSKI A., OSZCZEPALSKI S. and PIESTRZYŃSKI A. (1997) — Exploration for Cu-Ag and Au-Pt-Pd Kupferschiefer-type deposits in SW Poland. In: Mineral Deposits (ed. H. Papunen): 119–122.

SULLIVAN M. D., HASZELDINE R. S. and FALLICK A. E. (1990) — Linear coupling of carbon and strontium isotopes in Rotliegend Sandstone, North Sea: evidence for cross-formational fluid flow. Geology, **18**: 1215–1218.

SUN Y. (1998) — Influences of secondary oxidation and sulfide formation on several maturity parameters in Kupferschiefer. Org. Geochem., **29**: 1419–1429.

SUN Y. and PÜTTMANN W. (1997) — Metal accumulation during and after deposition of the Kupferschiefer from the Sangerhausen Basin, Germany. Appl. Geochem., **12**: 577–592.

SUN Y., PÜTTMANN W. and SPECZIK S. (1995) — Differences in the depositional environment of basal Zechstein in southwest Poland: implication for base metal mineralization. Org. Geochem., **23**: 819–835.

TAYLOR G. H., TEICHMÜLLER M., DAVIS A., DIESSEL C. F. K., LITTKE R. and ROBERT R. (1998) — Organic Petrology. Gebrüder Borntraeger.

TEICHMÜLLER M. (1986) — Organic petrology of source rocks, history and state of the art. Org. Geochem., **10**: 581–599.

TEICHMÜLLER M. and DURAND B. (1983) — Fluorescence microscopical rank studies on liptinites and vitrinites in peat and coals, and comparison with the results of the Rock-Eval pyrolysis. Int. J. Coal Geol., **2**: 197–230.

TEICHMÜLLER M. and OTTENJANN C. (1977) — Art, und Diagenese von Liptiniten und lipoiden Stoffen in einem Erdölmuttergestein auf Grund fluorescenz mikroskopischer Untersuchungen. Erd. Kohle, **30**: 387–398.

TISSOT B. P. and WELTE D. H. (1984) — Petroleum formation and occurrences. Springer Berlin.

TONN H., SCHMIDT F.-P., PORADA H. and HORN E.-E. (1987) — Untersuchungen von Fldssigkeitseinschldssen im Zechstein als Beitrag zur Genese des Kupferschiefers. Fortschr. Mineral., 65, Suppl. **1**.

van WEES J.-D., STEPHENSON R. A., ZIEGLER P. A., BAYER U., Mc CANN T., DADLEZ R., GAUPP R., NARKIEWICZ M., BITZER F. and SCHECK M. (2000) — On the origin of the Southern Permian Basin, Central Europe. Marine Petrol. Geol., **17**: 43–59.

VAUGHAN D. J., SWEENEY M., FRIEDRICH G., DIEDEL R. and HARAŃCZYK C. (1989) — The Kupferschiefer: An overview with an appraisal of the different types of mineralization. Econ. Geol., **84**: 1003–1027.

WODZICKI A. and PIESTRZYŃSKI A. (1994) — An ore genetic model for the Lubin-Sieroszowice mining district, Poland. Mineral. Deposita, **29**: 30–43.

WOLF M., DAVID P., ECKARDT C. B., HAGEMANN H. W. and PÜTTMANN W. (1989) — Facies and rank of the Permian Kuperschiefer from the Lower Rhine Basin and NW Germany. Int. J. Coal Geol., **14**: 119–136.

WOOD S. C., MOUNTAIN B. W. and PAN P. (1992) — The aqueous geochemistry of platinum, palladium and gold: recent experimental constraints and a re-evaluation of theoretical predictions. Can. Mineral., **30**: 955–982.

YANAGISAWA F. and SAKAI H. (1983) — Preparation of SO_2 for sulfur isotope ratio measurement by thermal decomposition of $BaSO_4$-V_2O_5-SiO_2 mixtures. Anal. Chem., **55**: 985–998.

YAWANARAJAH S. R., KRUGE M. A., MASTALERZ M. and ŚLIWIŃSKI W. (1993) — Organic geochemistry of Permian organic-rich sediments from the Sudetes area, SW Poland. Org. Geochem., **20**: 67–281